

Universal solvent quality crossover of the zero shear rate viscosity of semidilute DNA solutions

Sharadwata Pan,^{1,2,3} Duc At Nguyen,³ P. Sunthar,^{2,1} T. Sridhar,^{3,1} and J. Ravi Prakash^{3,1, a)}

¹⁾*IITB-Monash Research Academy, Indian Institute of Technology Bombay, Powai, Mumbai - 400076, India*

²⁾*Department of Chemical Engineering, Indian Institute of Technology Bombay, Powai, Mumbai - 400076, India*

³⁾*Department of Chemical Engineering, Monash University, Melbourne, VIC 3800, Australia*

(Dated: 8 November 2019)

The radius of gyration and the hydrodynamic radius of a number of linear, double-stranded DNA molecules, ranging in length from 3 to 300 kilobase pairs, extracted from modified strains of *E. coli* and dissolved in the presence of excess salt in a commonly used solvent, have been obtained by static and dynamic light scattering measurements. Using scaling relations from polymer solution theory, the θ -temperature for this solvent, and the crossover swelling of the two radii have been determined. It is shown that, as in the case of neutral synthetic polymer solutions, dilute DNA solutions exhibit universal swelling behaviour. Comparison of the universal swelling with previously obtained results of Brownian dynamics simulations enables an estimate of the solvent quality of a DNA solution at any temperature and molecular weight. The zero shear rate viscosity of semidilute unentangled DNA solutions, measured across a range of molecular weights and concentrations at a fixed value of solvent quality, is shown to obey power law scaling with concentration predicted by scaling theory, but with an effective exponent ν_{eff} that depends on the solvent quality, in place of the Flory exponent ν .

PACS numbers: 61.25.he, 82.35.Lr, 83.80.Rs, 87.14.gk, 87.15.hp, 87.15.N-, 87.15.Vv

Keywords: Semidilute polymer solution; static and dynamic light scattering; DNA solution, zero shear rate viscosity, solvent quality

^{a)}Corresponding author: ravi.jagadeeshan@monash.edu

I. INTRODUCTION

The rheological behaviour of semidilute solutions of linear uncharged polymers has not been as extensively characterised experimentally or theoretically as the behaviour of dilute and concentrated solutions. The most successful description so far of the equilibrium static and dynamic properties of semidilute polymer solutions comes from scaling theories that are based on the concept of a “blob” [de Gennes, 1979; Doi and Edwards, 1986; Grosberg and Khokhlov, 1994; Rubinstein and Colby, 2003]. Indeed results of recent investigations of the rheological behaviour of semidilute solutions have been interpreted within this framework [Heo and Larson, 2005, 2008]. It should be noted, however, that power law descriptions of scaling behaviour derived from blob theory are expected to be valid only in the limits of θ and very good solvents. More recently, the development of advanced mesoscopic simulation techniques that are capable of capturing the many body interactions between segments of the polymer chains has enabled the simulation of the behaviour of semidilute solutions for the first time [Ahlricks *et al.*, 2001; Huang *et al.*, 2010; Stoltz *et al.*, 2006]. The use of a repulsive pair-wise excluded volume potential between polymer segments in these simulations, however, implies that their results are restricted to the good solvent regime. The rheological behaviour of semidilute solutions in the crossover regime between θ and good solvents has consequently not been systematically studied so far. In this paper, we carefully experimentally investigate this regime and examine in particular if the zero shear rate viscosity exhibits universal scaling behaviour.

Semidilute solutions of DNA have been used to carry out the studies reported here. DNA is a polyelectrolyte, but under high salt conditions behaves like a charge neutral worm-like chain with a persistence length of about 50 nm [Barrat and Joanny, 1996; Bustamante *et al.*, 1994; Marko and Siggia, 1995; Robertson *et al.*, 2006; Smith *et al.*, 1996a; Sorlie and Pecora, 1990]. The monodispersity of DNA and its ability to be stained for visualization has made it an excellent candidate for studying the static and dynamic properties of polymer solutions, both at and far from equilibrium and at a range of concentrations [Fujimoto *et al.*, 1994; Hodnett *et al.*, 1976; Laib *et al.*, 2006; Marathias *et al.*, 2000; Nayvelt *et al.*, 2007; Nicolai and Mandel, 1989; Pecora, 1991; Ross and Scruggs, 1968; Sibileva *et al.*, 1987; Smith and Chu, 1998; Valle *et al.*, 2005]. It has consequently been used extensively for a variety of experimental measurements. For instance, measurements have been made of the diffusivity [Chirico *et al.*, 1989; Fishman and Patterson, 1996; Langowski, 1987; Robertson *et al.*, 2006; Selis and Pecora, 1995; Smith *et al.*, 1996b],

intrinsic viscosity [Doty *et al.*, 1958; Leighton and Rubenstein, 1969], relaxation times in semidilute solutions [Hur *et al.*, 2001; Liu *et al.*, 2009], extensional viscosity [Sunthar *et al.*, 2005] and conformational evolution in cross-slot flows [Babcock *et al.*, 2003; Schroeder *et al.*, 2003]. In all these experimental observations, the precise quality of the solvents that were used has not been reported. However, in order to characterise the crossover behaviour of semidilute solutions, it is essential to determine both the θ -temperature, and the solvent quality of the solution at any temperature above the θ -temperature.

In this paper, we find the θ -temperature of a DNA solution with the help of static and dynamic light scattering measurements. The methodology for determining the solvent quality of the solution is also established by systematically characterising DNA molecules in an extended range of molecular weights from 3–300 kilobase pairs (kbp) ($\approx 10^6$ – 10^8 daltons), and at a variety of different temperatures. Basically, we show that, similar to the behaviour exhibited by charge neutral synthetic polymer solutions, the swelling of DNA solutions in excess salt also exhibits universal behaviour in the context of two properties: (i) the swelling of the radius of gyration (R_g), which is a static equilibrium property, and (ii) the swelling of the hydrodynamic radius (R_H), which is a dynamic equilibrium property. By superimposing the experimental master curves on exact Brownian dynamics simulations predictions of the swelling, the solvent quality of the solution at any given temperature and DNA molecular weight is determined.

With the solvent quality determined, measurements of the zero shear rate viscosity have been carried out for DNA of different molecular weights, and at different temperatures, ensuring that all solutions have identical solvent qualities. We find that the dependence of zero shear rate viscosity on concentration is in perfect agreement with the power law scaling predicted by blob theory in the limits of θ and very good solvents. More interestingly, we show that the behaviour in the crossover regime can also be represented by power laws in terms of an effective exponent ν_{eff} that depends on the solvent quality.

The plan of the paper is as follows. In the next section, we briefly describe the protocol for our experiments, with details deferred to the supporting information. The procedure used here to determine the solvent quality of a DNA solution is discussed in section III, with a subsection on the method adopted here for determining the θ temperature of the solution (III A), and another in which the swelling of DNA is compared to previously reported swelling of charge neutral synthetic polymers and to the results of prior predictions by Brownian dynamics simulations (III B). In section IV, the concentration dependence of the zero shear rate viscosity in dilute and semidilute

solutions is reported, and the existence of universal crossover behaviour in the semidilute regime is demonstrated. A comparison of the persistence length of DNA measured here with several earlier observations is reported in Appendix A, and the reliability of the current measurements under poor solvent conditions is discussed in Appendix B. Our conclusions are summarised in section V.

II. METHODOLOGY

A. Light scattering

In order to experimentally characterize the properties of double-stranded DNA, a range of large molecular weight DNA, each with a monodisperse population, is desirable. The present work is greatly facilitated by the work of Smith’s group [Laib *et al.*, 2006] who genetically engineered special double-stranded DNA fragments in the range of 3–300 kbp and incorporated them inside commonly used *Escherichia coli* (*E. coli*) bacterial strains. These strains can be cultured to produce sufficient replicas of its DNA, which can be cut precisely at desired locations to extract the special fragments.

The *E. coli* stab cultures were procured from Smith’s group and the DNA fragments were extracted, linearized and purified according to standard molecular biology protocols [Laib *et al.*, 2006; Sambrook and Russell, 2001]. The various DNA fragments used here are listed in Table I of the supplementary material. In addition to the DNA samples procured from Smith’s group, two low molecular weight DNA samples (2.9 and 8.3 kbp), procured from Santosh Noronha’s laboratory at IIT Bombay, have been used in the light scattering measurements. The supplementary material also includes details of working conditions, procedures for preparation and quantification of linear DNA fragments, particulars of the dynamic and static light scattering measurements, and the approach used here for the determination of second virial coefficients.

For each molecular weight, the purified linear DNA pellet was dissolved in a solvent (Tris-EDTA Buffer), which is commonly used in physics [Robertson *et al.*, 2006; Smith and Chu, 1998; Smith *et al.*, 1996a] and rheology [Sunthar *et al.*, 2005] experiments. It contains 0.5 M NaCl, which we establish shortly below is above the threshold for observing charge-screening effects [Marko and Siggia, 1995]. Consequently, the DNA molecules are expected to behave identically to neutral molecules. The detailed composition of the solvent is given in Table II of the supplementary material.

We have used Static Light Scattering (SLS) (BI-200SM Goniometer, Brookhaven Instruments Corporation, USA) to determine R_g and the second virial coefficient A_2 at different temperatures (from 10–35°C), and dynamic Light Scattering (DLS) (Zetasizer Nano ZS, Malvern, UK) has been employed to determine R_H at different temperatures (from 5–35°C). A concentration of $c/c^* = 0.1$ (for DLS) and $c/c^* = 0.05$ –0.1 (for SLS) has been used throughout this study. Note that, $c^* = \frac{M}{N_A(4\pi/3)R_g^3}$, is the overlap concentration, calculated based on the measured values of R_g , with N_A being the Avogadro number. Typical c^* values for different DNA molecular weights are listed in Table III of the supplementary material. Initial estimates of c^* were based on values of R_g suggested in Laib *et al.* [2006] for molecular weights that are identical to those used in this study.

B. Rheometry

The viscosity measurements reported here have been carried out on three different DNA molecular weight samples, (i) 25 kbp, procured from Smith’s group as described above, (ii) linear genomic DNA of λ -phage (size 48.5 kbp), purchased from New England Biolabs, U.K. (#N3011L), and (iii) linear genomic DNA of T4 phage (size 165.6 kbp), purchased from Nippon Gene, Japan (#314-03973).

All measurements were carried out with a Contraves Low Shear 30 with cup and bob geometry (1T/1T). This instrument is efficient for measuring low viscosities and has very low zero-shear rate viscosity sensitivity at a shear rate of 0.017 s^{-1} [Heo and Larson, 2005]. The measuring principle of this device is detailed in an earlier study [Heo and Larson, 2005]. The primary advantage of using this is a small sample requirement (minimum 0.8 ml), which is ideal for measuring DNA solutions. The zero error was adjusted prior to each measurement. The instrument was calibrated with appropriate Newtonian Standards with known viscosities (around 10, 100 and 1000 mPa-s at 20°C) before measuring actual DNA samples. Values obtained fall within 5% of the company specified values.

Steady state shear viscosities were measured at a temperature range of 10 to 35°C for all linear DNA samples and a continuous shear ramp was avoided. Prior to measurements, λ and T4 DNA were kept at 65°C for 10 minutes and immediately put in ice for 10 minutes for their maximum concentrations. This was done to prevent aggregation of long DNA chains [Heo and Larson, 2005]. The shear rate range of the instrument under the applied geometry is from 0.01 to 100 s^{-1} . At each shear rate, a delay of 30 seconds was employed so that the DNA chains get ample time to

relax to their equilibrium state. At each temperature, a 30 minutes incubation time was employed for sample equilibration.

The shear viscosities at each temperature and concentration in the plateau (very low shear rate) region were least-square fitted (along with the errors) with straight lines and extrapolated to zero shear rate. The zero shear rate viscosities were determined in this manner for the different molecular weight DNA samples.

III. DETERMINATION OF THE SOLVENT QUALITY OF A DNA SOLUTION

In all experimental observations carried out so far on DNA solutions in excess salt, it is implicitly assumed that their behaviour is identical to the behaviour of neutral polymer solutions. Indeed all experimental observations so far support this implicit assumption in terms of general expectations of their behaviour. However, a unique aspect of solutions of synthetic polymers of sufficiently large molecular weight, namely, the existence of universal behaviour due to the self-similar character of polymer molecules, has not been investigated for DNA solutions. Universal behaviour enables the representation of experimental observations in terms of master plots, and the description of solution behaviour in terms of scaling variables.

An example of universal behaviour in the dilute limit that is of relevance to this work is that exhibited by the swelling of individual polymer chains when the polymer solution temperature T increases above the θ temperature, T_θ , due to repulsive intramolecular interactions. Such expansion is well described by dimensionless expansion (or swelling) ratios [Rubinstein and Colby, 2003], for instance, α_g for R_g and α_H for R_H :

$$\alpha_g = \frac{R_g(T)}{R_g^\theta} \quad (1)$$

$$\alpha_H = \frac{R_H(T)}{R_H^\theta} \quad (2)$$

where, $R_g(T)$ and $R_H(T)$ are the radius of gyration and the hydrodynamic radius at any temperature $T > T_\theta$, and R_g^θ and R_H^θ represent the θ -temperature values of these quantities. As is well known, while the scaling of the radius of gyration and the hydrodynamic radius with molecular weight M obeys universal power laws in the special cases of θ , athermal, and non-solvents, in the intermediate crossover region between θ and athermal solvents, the ratios α_g and α_H can be collapsed onto master plots when plotted in terms of a single scaling variable, $\tau = \left(1 - \frac{T_\theta}{T}\right) \sqrt{M}$, that

combines the dependence on temperature and molecular weight [Hayward and Graessley, 1999; Rubinstein and Colby, 2003].

In the case of neutral synthetic polymer solutions, this universal behaviour is commonly interpreted in terms of the two-parameter theory [Miyaki and Fujita, 1981; Yamakawa, 2001]. According to the two-parameter theory, the values of properties at any temperature T under good solvent conditions, can be expressed as an unique function of just two parameters, namely, the radius of gyration under θ conditions, R_g^θ , and a solvent quality parameter, commonly denoted by z [Schäfer, 1999]. The parameter z is proportional to the square root of the number of monomers in the polymer chain, with the proportionality constant being related to the binary cluster integral, which reflects the departure of the temperature from the θ -temperature, and the chemistry of solvent-mediated interactions between monomers in different parts of the chain [Rubinstein and Colby, 2003; Yamakawa, 2001]. Thus, for instance,

$$R_g(T) = R_g^\theta f_g(z) \quad (3)$$

implying the universal two-parameter theory prediction, $\alpha_g = f_g(z)$, where f_g is a universal function of z , whose specific form will be elaborated later. Similar predictions are made by two-parameter theory for α_H and the swelling of the viscometric radius R_v , which is based on the intrinsic viscosity [Hayward and Graessley, 1999]. The connection between universal two-parameter theory predictions and the master plots obtained by experiments on synthetic polymer solutions has been made by relating z to the scaling variable τ through a simple linear relation $z = k\tau$, where k is a constant that depends on polymer-solvent chemistry [Hayward and Graessley, 1999; Schäfer, 1999].

Away from equilibrium, a scaling variable in addition to z is required to characterize dilute solution behaviour. For instance in shear flows, it has been found that including a characteristic shear rate β enables the representation of rheological behaviour in terms of universal plots [Kumar and Prakash, 2004; Prakash, 2002], while in extensional flows, the inclusion of the Weissenberg number Wi enables a similar representation [Sunthar and Prakash, 2005]. Indeed, a quantitative comparison of the stretch evolution of DNA in a cross slot flow [Smith and Chu, 1998], and the extensional viscosity of DNA solutions in uniaxial elongational flow [Sunthar *et al.*, 2005] was shown to be possible once an estimate of the solvent quality z of the solution was made. However, to the best of our knowledge, a systematic study to estimate the solvent quality of DNA solutions has not been attempted so far. The characterization of DNA solutions in terms of the two-

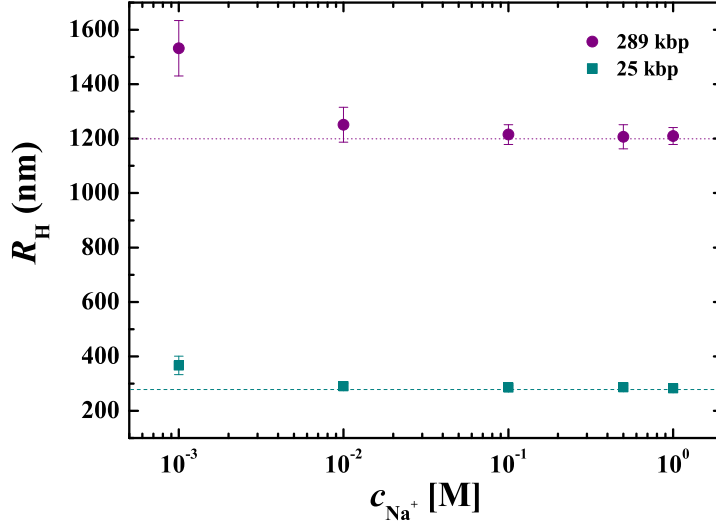


FIG. 1. Dependence of R_H on salt concentration for two different molecular weights at 25 °C.

parameter theory would provide a powerful predictive tool for theoretical analysis of its dynamics in equilibrium and in flow.

In order to proceed with the experiments proposed in this work, it is essential to first establish the salt concentration regime in which DNA (a polyelectrolyte) behaves as a neutral polymer. We have measured the hydrodynamic radius of two different linear DNA fragments across a range of salt concentrations (from 0.001 to 1 M) at 25°C and the results are displayed Figure 1. It is clear from the figure that complete charge screening occurs above 10 mM NaCl. This is in agreement with earlier dynamic light scattering studies on linear DNA [Langowski, 1987; Liu *et al.*, 2000; Soda and Wada, 1984]. Since the solvent used here contains 0.5 M NaCl, the light scattering experiments of the current study are in a regime well above the threshold for observing charge screening effects. We have also determined the persistence length of DNA under conditions where the charges are completely screened, and our estimate agrees with earlier measurements of the persistence length under such conditions. These results are discussed in Appendix A.

Figure 2 compares present measurements of the dependence of hydrodynamic radius on molecular weight with previous measurements [Robertson *et al.*, 2006; Smith *et al.*, 1996a] at 25°C. While Smith *et al.* [1996a] used fragments and concatenates of λ phage DNA to obtain molecules across the wide range of molecular weights that were studied, the measurements of Robertson *et al.* [2006] were carried out on molecules identical to those that have been used here.

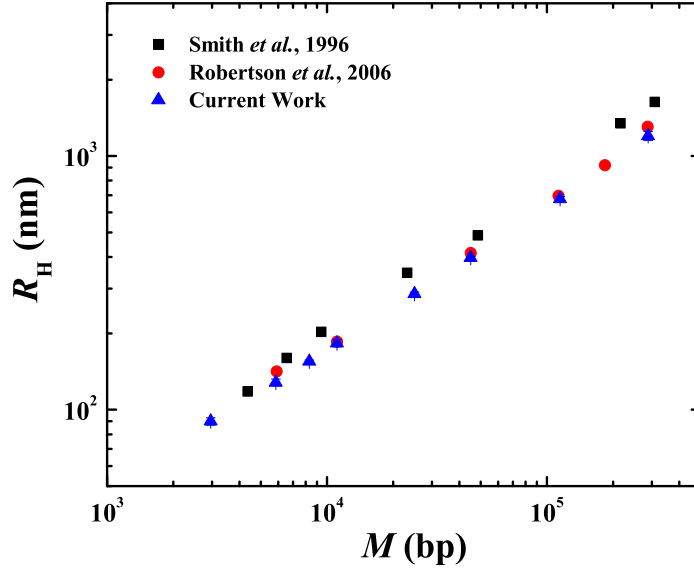


FIG. 2. Comparison of the molecular weight dependence of hydrodynamic radius, obtained previously by Smith *et al.* [1996a] and Robertson *et al.* [2006] at 25°C with the current work.

These results were used by Smith and co-workers to demonstrate that double-stranded DNA in solutions with excess salt obey the molecular weight scaling expected from polymer solution theory in the presence of excluded volume interactions. In the present work, we extend the measurements to a wide range of temperatures in order to carry out a systematic study of the crossover region between θ and very good solvents.

A. The θ -temperature

The θ -temperature for a particular polymer-solvent pair can be inferred from the measured data, by several signatures. We have employed two methods—molecular weight scaling and the second virial coefficient transition. At the θ -temperature, R_g and R_H scale as $M^{0.5}$ for large molecular weight linear polymers. With this expected behaviour, two dimensionless scaling variables can be defined:

$$\Pi_g \equiv \frac{R_g}{a \sqrt{M}} \quad (4)$$

$$\Pi_H \equiv \frac{R_H}{a \sqrt{M}} \quad (5)$$

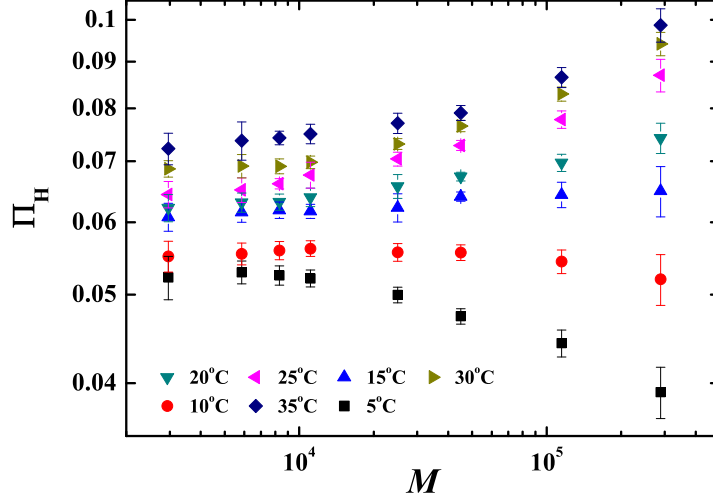


FIG. 3. Scaled hydrodynamic radius (Π_H) as a function of molecular weight in base-pairs or bp. Slopes are calculated at each temperature by a least-squares linear fit of the last four data points.

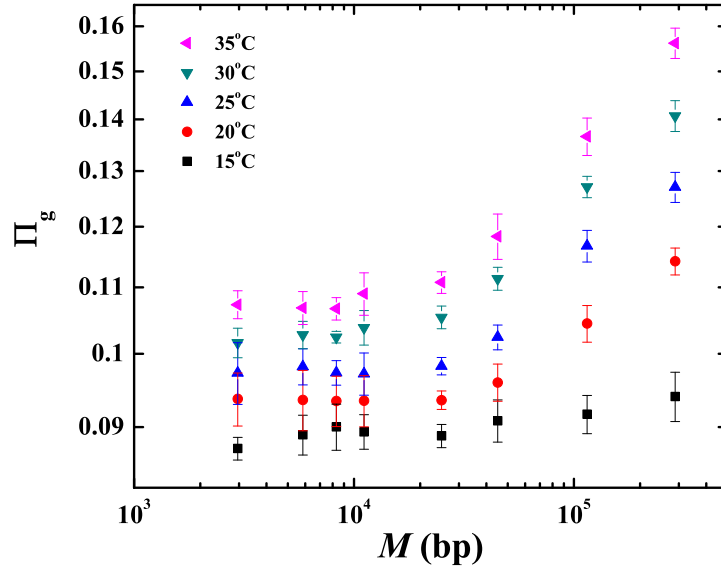


FIG. 4. Scaled radius of gyration (Π_g) as a function of molecular weight in bp. Slopes are calculated at each temperature by a least-squares linear fit of the last four data points.

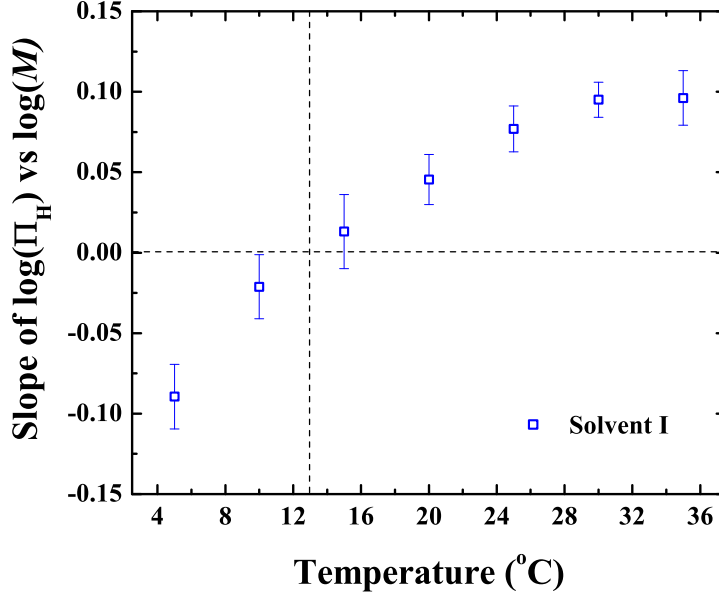


FIG. 5. Variation of slope obtained from Figure 3 with temperature. Readings corresponding to 5 to 25°C are fitted with a second order polynomial to calculate the θ -temperature.

where, a is a constant with dimensions of length, which we have set equal to 1 nm. Both Π_H and Π_g should increase with molecular weight for good solvents, remain constant for theta solvents, and decrease for poor solvents.

Figures 3 and 4 show Π_H and Π_g plotted against M in log-log plots. In line with expectation, the data shows a monotonic trend: decreasing with molecular weight for certain temperatures, remaining relatively constant at intermediate temperatures, and increasing with M for higher temperatures. In order to determine the θ -temperature precisely, the *effective* slope of the curves at sufficiently large molecular weights was plotted against absolute temperature and fitted either with a second order polynomial or subjected to linear interpolation. The temperature where the sign of the slope changes from negative to positive, is taken to be T_θ . A value of $T_\theta = 13 \pm 2$ °C was estimated for the DNA-Solvent pair, after taking into account experimental errors in Π_g or Π_H (see Figure 5).

Figures 3 and 4 also indicate that for the relatively *smaller* molecular weight samples, at all the observed temperatures, both Π_H and Π_g are roughly constant with increasing molecular weight. This behaviour is consistent with the *blob* scaling argument which anticipates that below a length

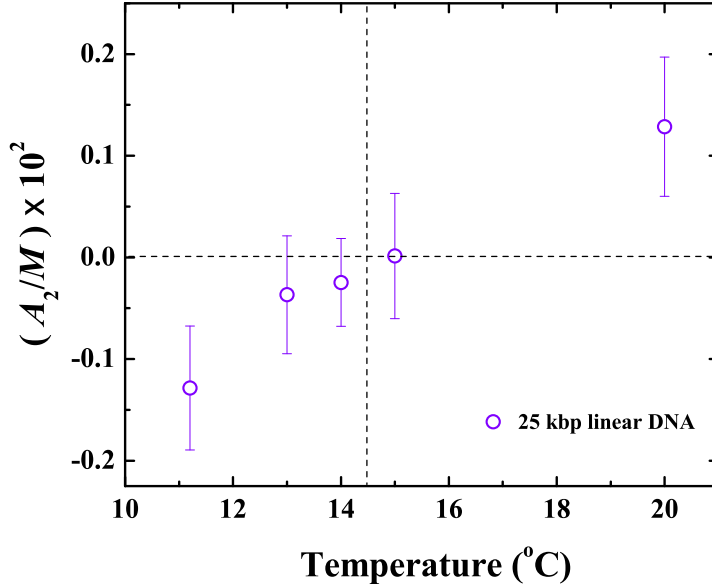


FIG. 6. Variation with temperature of the ratio of second virial coefficient to molecular weight. Data points are least-squares linear-fitted to calculate the θ -temperature.

scale corresponding to a *thermal* blob, the energy of excluded volume interactions is less than $k_B T$ (where k_B is the Boltzmann constant), as a result of which chain segments with size less than the blob size obey ideal chain statistics, and scale as $M^{0.5}$ at all temperatures Rubinstein and Colby [2003]. In Appendix B, we exploit the consequences of this scaling argument to determine the size of thermal blobs as a function of temperature in DNA solutions, under good and poor solvent conditions.

An alternative method employed in synthetic polymer literature for estimating the theta temperature is by determining the second virial coefficient A_2 [Krigbaum, 1954; Orofino and Mickey Jr., 1963; Shultz and Flory, 1952], either from the concentration dependence of osmotic pressure, light scattering from dilute polymer solutions, or by measuring intrinsic viscosities of dilute polymer solutions. A_2 is a direct measure of excluded volume interactions between pairs of chains [Rubinstein and Colby, 2003]. In this work, a quantity that is linearly proportional to the second virial coefficient is determined for a single, linear, medium molecular weight DNA fragment (25 kbp) by static light scattering, according to the procedure described in Orofino and Mickey Jr. [1963]. The exact values of A_2 are not determined since we are interested only in the tempera-

ture where it vanishes. The sign of A_2 , which is indicative of repulsion or attraction between the segments of a chain [Rubinstein and Colby, 2003], is positive in good solvents, negative in a poor solvents and vanishes at the theta temperature. The temperature at which A_2 vanishes, determined by interpolating the measured data, is used here as an estimate of T_θ , as shown in Fig. 6. We find $T_\theta = 13 \pm 2$ °C for the solvent used in this study. This value agrees, within experimental error, with the value obtained using the molecular weight scaling method.

Once the value of T_θ has been determined, the values of R_H^θ and R_g^θ for all the molecular weights considered here can be evaluated from values of R_H and R_g measured at the various temperatures. In the case of R_H , since T_θ lies within the range of experimental temperatures, R_H^θ can be obtained by linear interpolation. On the other hand, since T_θ lies outside the range of experimental temperatures for the R_g measurements, R_g^θ can be obtained by linearly extrapolating values of R_g measured at a fixed molecular weight and at different temperatures $T > T_\theta$, to the value of T_θ . Figure 7 demonstrates this procedure for two different molecular weights, using values of R_g measured at various temperatures. The values of R_H^θ and R_g^θ determined by this procedure are plotted against M in Figure 8, which confirms that indeed ideal chain statistics are obeyed at the estimated θ -temperature. Estimated values of R_H^θ and R_g^θ for all the molecular weights considered here, are listed in Tables IV and V of the supplementary material.

Since the scaling of both R_g^θ and R_H^θ with M at the θ -temperature is the same ($M^{0.5}$), their ratio should be a constant. As is well known, experimental observations and theoretical predictions indicate that $U_{RD}^\theta = R_g^\theta/R_H^\theta$ is infact a chemistry independent universal constant (for a recent compilation of values see Table I in Kröger *et al.* [2000]). Zimm theory predicts a universal value $U_{RD}^\theta \approx 1.47934$ [Ottinger, 1996; Zimm, 1956]. Since we have estimated both R_g^θ and R_H^θ , we can calculate U_{RD}^θ for all the molecular weights used in this work. The molecular weight independence of U_{RD}^θ is shown in Figure 9. It is clear that the values obtained here are close to the value predicted by Zimm.

B. The universal swelling of DNA

In order to establish the universal nature of the swelling of DNA molecules in solution, it is sufficient to show that the data in the crossover region between θ and athermal solvents can be collapsed onto master plots when represented in terms of the scaling variable τ . However, it is more useful for comparisons between theories and experimental observations for DNA solution

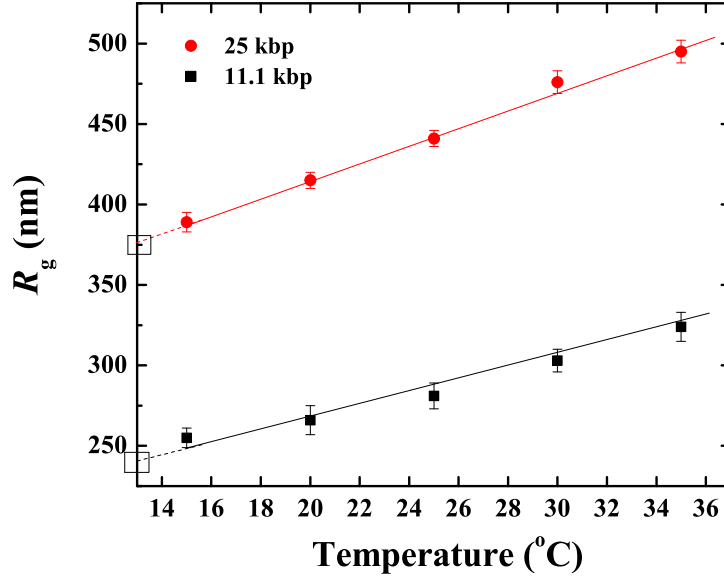


FIG. 7. Estimation of R_g^θ by extrapolation of R_g values measured at various temperatures to the value of $T_\theta = 13^\circ\text{C}$, for two different molecular weights.

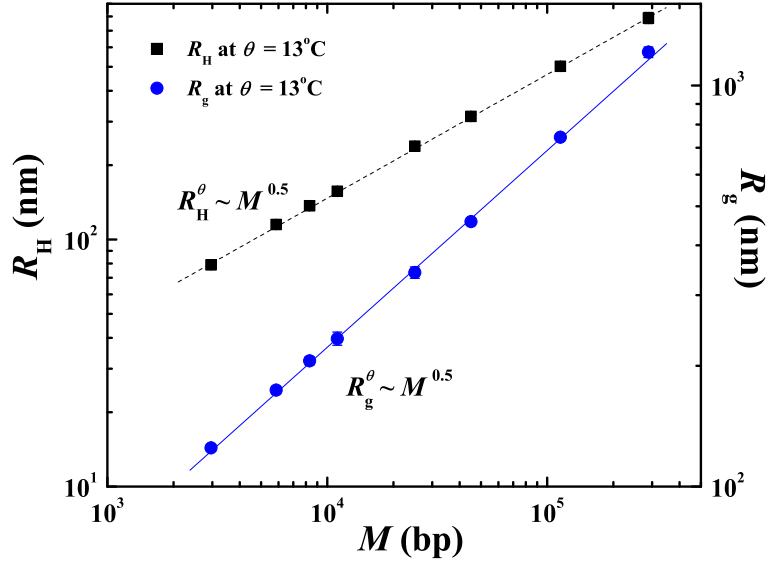


FIG. 8. The variation of the radius of gyration (R_g^θ) and the hydrodynamic radius (R_H^θ) with molecular weight (in bp) at the θ -temperature, which is estimated to be 13°C .

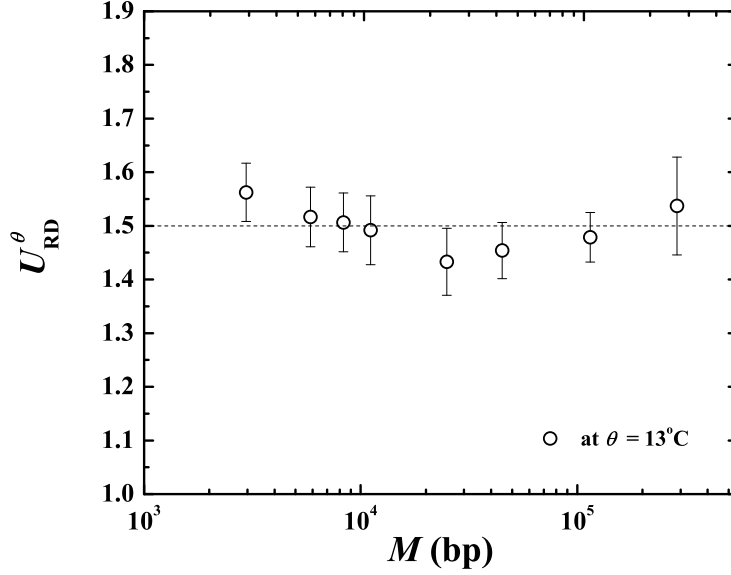


FIG. 9. The molecular weight independence of U_{RD}^θ . The values are in accordance with the Zimm model prediction of $U_{RD}^\theta \approx 1.47934$ in the long-chain limit [Ottinger, 1996; Zimm, 1956].

behaviour, if universal behaviour is established in a framework that enables such a comparison. As discussed earlier in section I, carrying out a systematic comparison of experimentally determined expansion factors with the predictions of two-parameter theory requires relating the scaling variable τ to the solvent quality parameter z , since theoretical predictions are made in terms of z .

Many versions of the two-parameter theory can be used for the purpose of comparison with experimental data. Early versions of the two-parameter theory, including Flory type *fifth power* theories, and theories based on perturbation expansions, are reviewed in the classic textbook by Yamakawa [2001]. The use of two-parameter theory to describe numerical results on self-avoiding walks on lattices is reviewed in Barrett *et al.* [1991]. While quantitative agreement between experiments and theory for the swelling of static properties such as the radius of gyration R_g can be obtained with the help of renormalization group theories [Schäfer, 1999], similar agreement has not been achieved for the swelling of the dynamic property R_H within this framework. Recently, quantitative predictions of both α_g and α_H have been achieved through the use of Brownian dynamics simulations [Kumar and Prakash, 2003; Sunthar and Prakash, 2006]. These simulations, which make use of a narrow Gaussian potential to represent excluded volume inter-

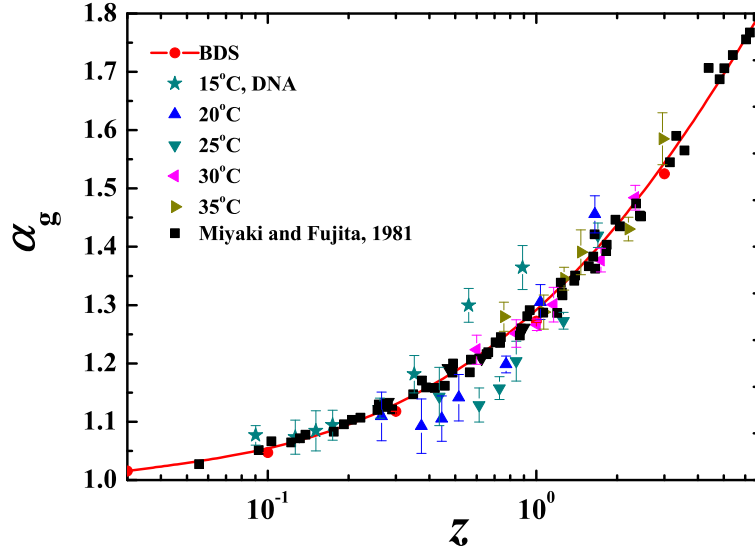


FIG. 10. Swelling of R_g vs z . The filled coloured symbols represent experimental data for DNA. BDS refers to the predictions of Brownian dynamics simulations [Kumar and Prakash, 2003], with the curve representing the function $f_g(z)$, with constants $a = 9.528$, $b = 19.48$, $c = 14.92$, and $m = 0.1339$. Black squares represent experimental data of polystyrene in cyclohexane and benzene, reproduced from Miyaki and Fujita, 1981 [Miyaki and Fujita, 1981].

actions (that enables controlled simulations in terms of the parameter z), give rise to parameter free predictions, independent of finite size effects, since they are based on the extrapolation of finite chain results to the long chain limit. In particular, the quantitative prediction of α_H was shown to require the inclusion of fluctuating hydrodynamic interactions [Sunthar and Prakash, 2006]. Interestingly, it turns out that lattice simulations, predictions of renormalization group theory, and results of Brownian dynamics simulations for the swelling of any typical generic property, say α , can be described by universal functions that have the functional form $\alpha = f(z)$, where, $f(z) = (1 + a z + b z^2 + c z^3)^{m/2}$, with the values of the constants a, b, c, m , etc., dependent on the particular theory adopted [Domb and Barrett, 1976; Kumar and Prakash, 2003; Schäfer, 1999]. Here, we choose to compare experimental results for α_g and α_H with the results of Brownian dynamics simulations, since they represent exact numerical simulations, and are not based on approximations unlike earlier analytical theories. The values of the various constants in the functions f_g and f_H that fit the results of Brownian dynamics simulations, are reported in the captions to Figs. 10

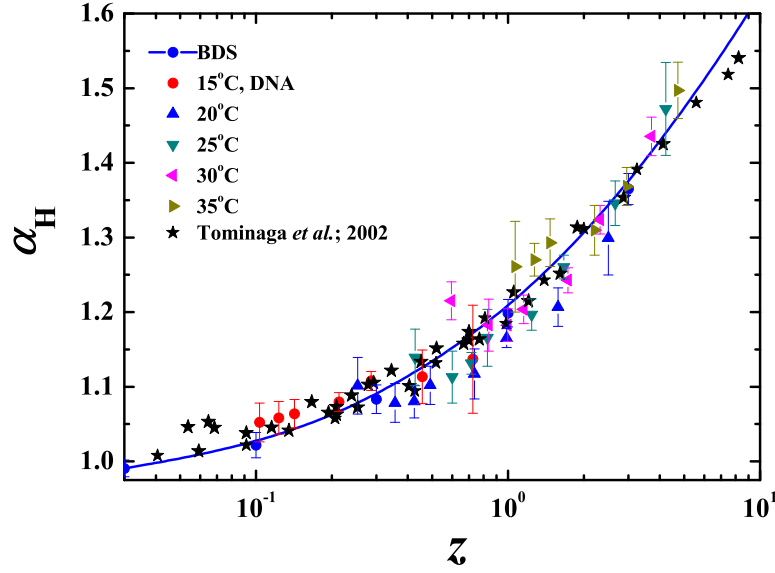


FIG. 11. Swelling of R_H vs z . The filled coloured symbols represent experimental data for DNA. BDS refers to the predictions of Brownian dynamics simulations [Sunthar and Prakash, 2006], with the curve representing the function $f_H(z)$, with constants $a = 9.528$, $b = 19.48$, $c = 14.92$, and $m = 0.067$. Black stars represent several experimental data on synthetic polymers collated in Tominaga *et al.* [2002].

and 11.

The chemistry dependent constant k that relates the value of z in Brownian dynamics simulations to the experimental value of τ remains to be determined. This is done as follows. Consider α_g^{expt} to be the experimental value of swelling at a particular value of temperature T and molecular weight M . It is then possible to find the Brownian dynamics value of z that would give rise to the same value of swelling, from the expression $z = f_g^{-1}(\alpha_g^{\text{expt}})$, where f_g^{-1} is the inverse of the function f_g . Since $z = k \hat{\tau} \sqrt{M}$, where $\hat{\tau} = \left(1 - \frac{T_\theta}{T}\right)$, it follows that a plot of $f_g^{-1}(\alpha_g^{\text{expt}}) / \sqrt{M}$ versus $\hat{\tau}$, obtained by using a number of values of α_g^{expt} at various values of T and M , would be a straight line with slope k . Once the constant k is determined, both experimental measurements of swelling and results of Brownian dynamics simulations can be represented on the same plot. As discussed in greater detail in the supplementary material, by using θ -temperature of 13°C for the solvent used in this study, the value of k , found by this procedure is $7.4 \times 10^{-3} \pm 3.0 \times 10^{-4}$. It follows that for any given molecular weight and temperature, the solvent quality z for the DNA solution can be determined.

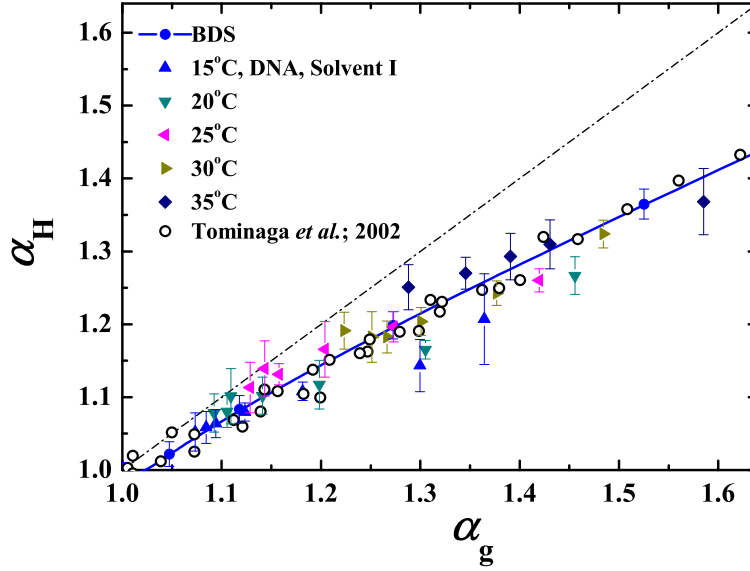


FIG. 12. Comparison of measured values of α_H against α_g . Filled symbols represent experimental data for DNA at good solvent conditions ($T > T_\theta$). BDS refers to the predictions of Brownian dynamics simulations [Sunthar and Prakash, 2006]. Open circles represent several experimental data on synthetic polymers collated in Tominaga *et al.* [2002].

The solvent quality crossover of α_g and α_H for DNA obtained by the procedure described above are shown in Figs. 10 and 11, along with Brownian dynamics simulations predictions. Experimental data of Miyaki and Fujita [1981] and Tominaga *et al.* [2002], which are considered to be highly accurate measurements of synthetic polymer swelling, are also plotted in the same figures. An alternative, z independent, means of presenting the swelling data is displayed in Fig. 12, where the values of α_g , at particular values of T and M , are plotted versus α_H at the same values of T and M . From these figures it is evident that, just as in the case of synthetic polymer solutions, irrespective of solvent chemistry, the swelling of DNA is universal in the crossover region between theta to good solvents. With the experimental swelling of DNA mapped onto theoretical predictions, it follows that other instances of universal behaviour, obtained for instance by simulations or theory for a particular value of z , can be compared with experimental results for DNA in the solvent used here, at the same value of z .

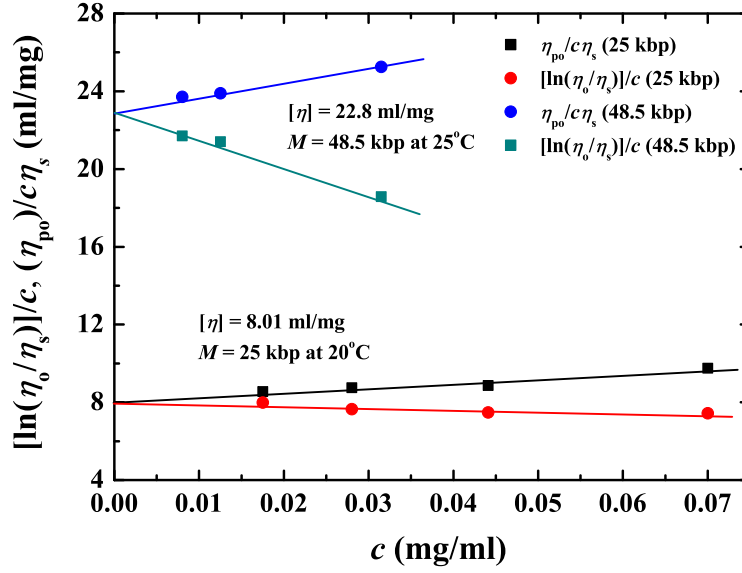


FIG. 13. Intrinsic viscosity of 25 kbp and λ DNA (48.5 kbp) at 20°C and 25°C, respectively, obtained by extrapolating data for $\ln(\eta_0/\eta_s)/c$ and $\eta_{p0}/c\eta_s$ at several finite concentrations to the limit of zero concentration.

IV. SOLVENT QUALITY CROSSOVER OF THE ZERO SHEAR RATE VISCOSITY

The intrinsic viscosity $[\eta]$ of the various DNA solutions used in this work has been obtained from the following two expressions,

$$[\eta] = \lim_{c \rightarrow 0} \frac{\ln(\eta_0/\eta_s)}{c}$$

$$[\eta] = \lim_{c \rightarrow 0} \frac{\eta_{p0}}{c\eta_s} \quad (6)$$

where, η_0 is the zero shear rate solution viscosity, η_s the solvent viscosity, and $\eta_{p0} = \eta_0 - \eta_s$, the polymer contribution to the zero shear rate solution viscosity. Essentially, data for $\ln(\eta_0/\eta_s)/c$ and $\eta_{p0}/c\eta_s$ obtained at several finite concentrations is extrapolated to the limit of zero concentration, as exemplified in Figure 13 for 25 kbp and λ DNA (48.5 kbp) at 20°C and 25°C, respectively. From the expression, $\eta = \eta_s [1 + [\eta]c + \dots]$, we expect that in the dilute regime ($c < c^*$),

$$\frac{\eta_{p0}}{\eta_s[\eta]c^*} = \frac{c}{c^*} \quad (7)$$

Figure 14 shows that indeed for all the temperatures measured here, both the 25 kbp and λ DNA samples exhibit a linear dependence on the scaled concentration c/c^* in the dilute regime.

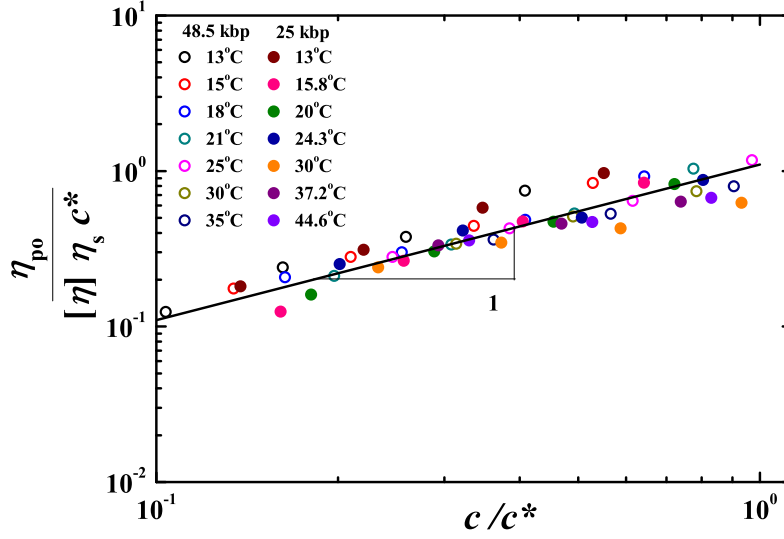


FIG. 14. Linear dependence of the viscosity ratio $\eta_{p0}/([\eta]\eta_s c^*)$ on the scaled concentration c/c^* , in the dilute solution regime, for 25 kbp and λ DNA (48.5 kbp) at a variety of different temperatures.

According to blob theory, the polymer contribution to the zero shear rate viscosity obeys the following scaling law in the semidilute unentangled regime in the limits of θ -solvents and very good solvents [Rubinstein and Colby, 2003],

$$\frac{\eta_{p0}}{\eta_s} \sim \left(\frac{c}{c^*} \right)^{1/(3\nu-1)} \quad (8)$$

where, the scaling exponent ν is equal to 0.5 in θ -solvents, and 0.588 in very good solvents. The semidilute unentangled regime is expected to span the range of concentrations from $c/c^* = 1$ to 10 [Graessley, 1980; Rubinstein and Colby, 2003]. Figure 15 displays the ratio η_{p0}/η_{p0}^* (where η_{p0}^* is the value of η_{p0} at $c = c^*$) at the θ -temperature estimated here. Using this ratio to represent the zero shear rate viscosity data ensures that $\eta_{p0}/\eta_{p0}^* = 1$ when $c/c^* = 1$ for all the systems studied here. The slope of 2 that is observed in the semidilute regime is consistent with the blob scaling law for $\nu = 0.5$. T4 DNA, which is the longest molecule in the series studied here, appears to follow the blob scaling for the largest concentration range. On the other hand, the 25 kbp and λ DNA seem to crossover into the entangled regime beyond a concentration $c/c^* \approx 3$.

The key result of the present work is displayed in Figure 16. The concentration dependence of three different molecular weights of DNA is presented for three different values of the solvent quality z . In order to maintain the same value of solvent quality across the various molecular weights,

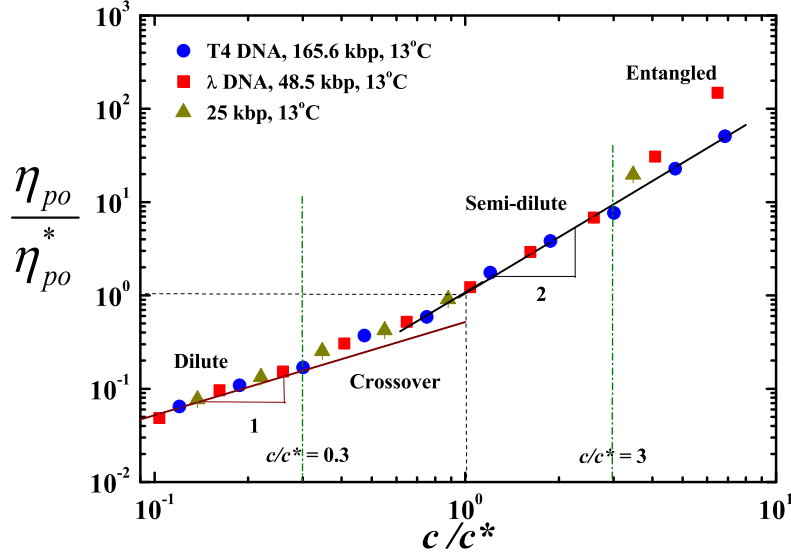


FIG. 15. Dependence of the viscosity ratio η_{p0}/η_{p0}^* (where η_{p0}^* is the value of η_{p0} at $c = c^*$) on the scaled concentration c/c^* , for 25 kbp, λ and T4 DNA, at the θ -temperature.

it is necessary to carry out the experiments at the appropriate temperature for each molecular weight. This procedure would not be possible without the systematic characterisation of solvent quality described earlier in section III. Remarkably, the data appear to collapse onto universal curves, independent of DNA molecular weight. Indeed the data appear to satisfy a power law analogous to the blob scaling power law,

$$\frac{\eta_{p0}}{\eta_s} \sim \left(\frac{c}{c^*}\right)^{1/(3\nu_{\text{eff}}(z)-1)} \quad (9)$$

where, ν_{eff} is an effective exponent that is a function of the solvent quality z . The value of $\nu_{\text{eff}}(z)$ can be extracted by equating the slope of the (η_{p0}/η_{p0}^*) versus (c/c^*) line in Figure 16 to $1/(3\nu_{\text{eff}} - 1)$, at each value of z . The effective exponent obtained in this manner can be compared to an alternative effective exponent that is commonly used to characterise the crossover from θ to good solvents [Schäfer, 1999].

Although the scaling of R_g with chain length N obeys a power law only in the limit of long chains, one can make the ansatz that, at all values of chain length, $R_g \sim N^{\nu_{\text{eff}}}$, with ν_{eff} representing an effective exponent that approaches its critical value as $N \rightarrow \infty$. It is straight forward then to show that,

$$\nu_{\text{eff}}(z) = \frac{1}{2} + \frac{1}{4} \frac{\partial \ln \alpha_g^2}{\partial \ln z}. \quad (10)$$

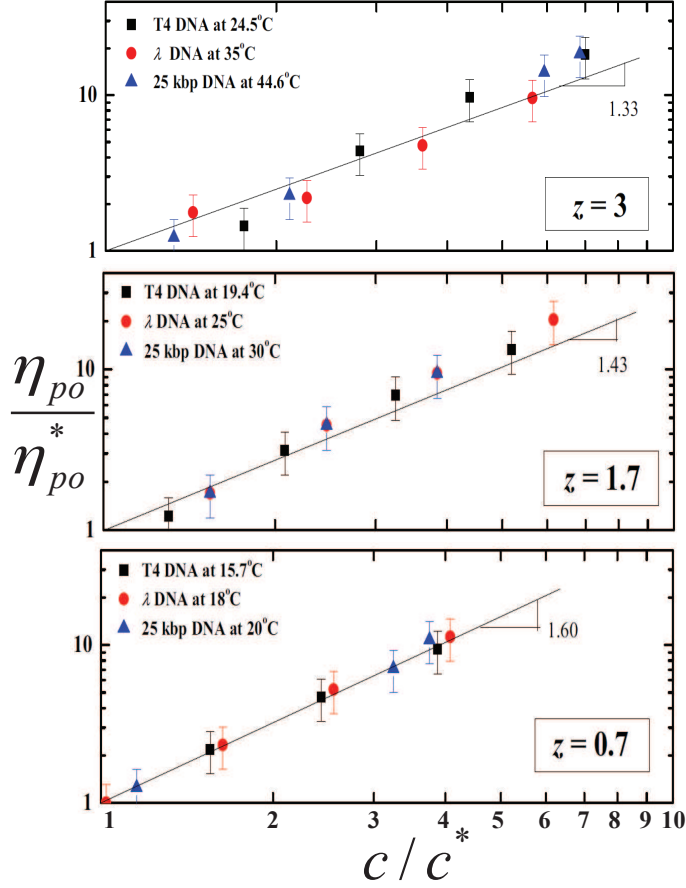


FIG. 16. Dependence of the viscosity ratio η_{p0}/η_{p0}^* on the scaled concentration c/c^* in the semidilute regime, for 25 kbp, λ and T4 DNA, at fixed values of the solvent quality z .

The curve fitting function for α_g^2 can consequently be suitably differentiated to obtain the z dependence of the effective exponent ν_{eff} . In an entirely analogous manner, one can make an ansatz regarding the scaling behavior of both α_H^2 and α_η^2 with N . Here, the swelling of the intrinsic viscosity is defined by the expression, $\alpha_\eta = ([\eta]/[\eta]_\theta)^{1/3}$, where $[\eta]_\theta$ is the intrinsic viscosity at the θ -temperature. The dependence of ν_{eff} on z in each of these cases, for the *exact* results of Brownian dynamics simulations, is illustrated in Figure 17. The black symbols represent the experimental values of ν_{eff} obtained from Figure 16 as described above. It is clear that the experimental ν_{eff} is bracketed by the three simulation estimates, with perhaps the closest proximity to the ν_{eff} versus z curve obtained from α_η^2 .

Liu *et al.* [2009] have recently examined the concentration dependence of the longest relaxation time λ_1 of semidilute solutions by studying the relaxation of stretched single T4 DNA molecules

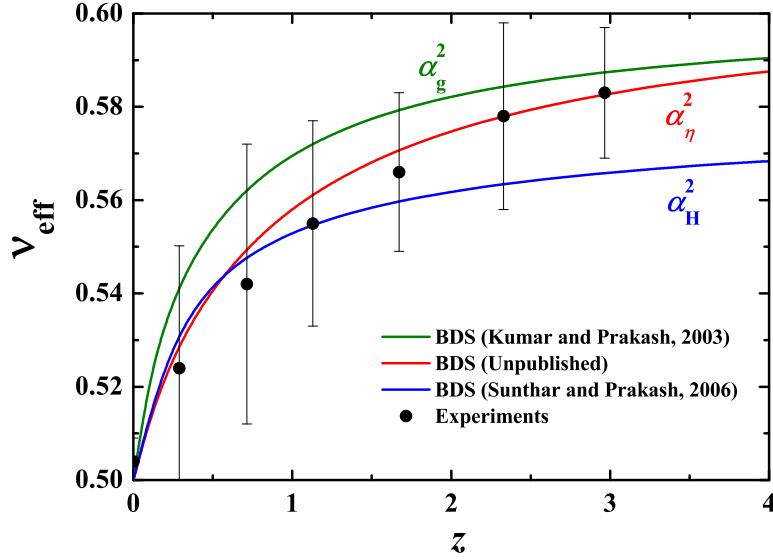


FIG. 17. Effective exponent ν_{eff} obtained from the universal crossover behaviour of α_g^2 , α_H^2 , and α_η^2 predicted by dilute solution Brownian dynamics simulations, compared with the effective exponent extracted from the crossover behaviour of the viscosity ratio in the semidilute regime (displayed in Figure 16). The simulation results for α_η^2 are reproduced from a currently unpublished work [Ahirwal *et al.*, 2012]

after extension. They find that the scaling of λ_1 in the semidilute unentangled regime obeys the power law expression predicted by blob theory,

$$\lambda_1 \sim \left(\frac{c}{c^*} \right)^{(2-3\nu)/(3\nu-1)} \quad (11)$$

It is common to define an alternative large scale relaxation time λ_η based on the zero shear rate viscosity η_{p0} by the following expression [Ottinger, 1996],

$$\lambda_\eta = \frac{M\eta_{p0}}{cN_A k_B T} \quad (12)$$

where, N_A is Avagadro's number and k_B is Boltzmanns constant. It is straight forward to show that in the semidilute unentangled regime λ_η obeys the same scaling with concentration as λ_1 . As a result, one expects the ratio λ_η/λ_1 to be independent of concentration. Indeed, in the dilute limit it is known that this ratio has a universal value, predictions of which range from 1.645 to 2.39 [Kröger *et al.*, 2000], depending on the theoretical approximation and solvent condition.

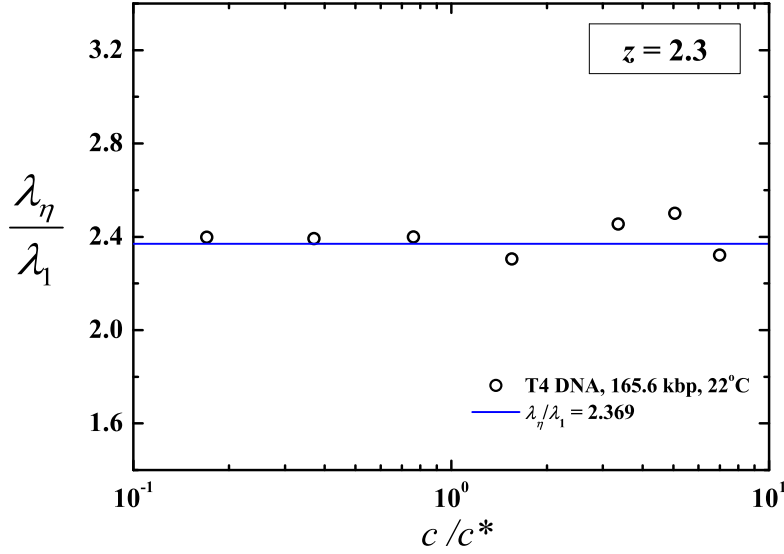


FIG. 18. Universal ratio of λ_1 (measured by Liu *et al.* [2009]) to λ_η (measured in the present work) for T4 DNA at a value of solvent quality $z = 2.3$, for a range of concentrations spanning the dilute and semidilute regime.

Since Liu *et al.* [2009] used the same solvent as the one used in the present study, it is possible to estimate the solvent quality of the T4 DNA solution used in their work, which we find to be $z = 2.3$. As a result, by using the value of η_{p0} measured at the same solvent quality, it is possible to find the ratio of λ_1 measured by Liu *et al.* [2009] to λ_η measured in the present work at $z = 2.3$. Results for this ratio at a range of concentrations are shown in Figure 18. Clearly the ratio has an universal value $\lambda_\eta/\lambda_1 \approx 2.369$ at $z = 2.3$, independent of concentration.

Recently, Somani *et al.* [2010] have predicted the dependence of the ratio λ_η/λ_1 on the solvent quality z in the dilute limit with the help of Brownian dynamics simulations. Their results are reproduced as the solid curve in Figure 19. Since λ_η/λ_1 does not depend on concentration, the same curve should be valid at all concentrations. It is possible therefore to compare the ratio λ_η/λ_1 estimated here with the results of [Somani *et al.*, 2010]. The red symbol in Figure 19 is the value of the ratio estimated here at $z = 2.3$. As can be seen, the estimated value is reasonably close to the simulation prediction at this value of z .

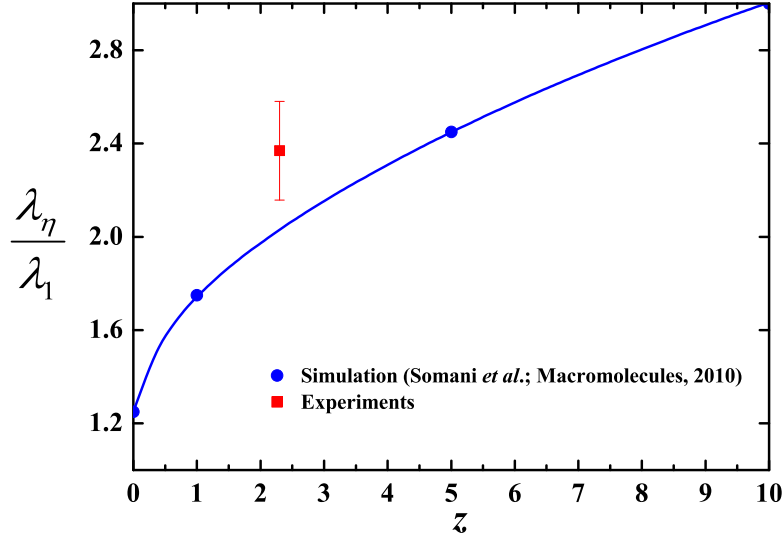


FIG. 19. Dependence of the ratio λ_η/λ_1 on the solvent quality z in the dilute limit predicted by Somani *et al.* [2010] with the help of Brownian dynamics simulations (solid curve). The red symbol is the value of the ratio estimated here at $z = 2.3$ using the value of λ_1 measured by Liu *et al.* [2009] and λ_η measured in the present work.

V. CONCLUSIONS

Static and dynamic properties of DNA in a commonly used buffer solution have been characterized in terms of parameters used in dilute polymer solution theory. Using known scaling relationships from polymer solution theory, the θ -temperature (T_θ) in this solvent and the crossover of the swelling of the two radii in good solvent conditions ($T > T_\theta$) were determined. DNA in this solvent (10 mM Tris, 1 mM EDTA, 0.5 M NaCl) has $T_\theta = 13 \pm 2^\circ\text{C}$. As with the regular polymers, the dilute solution crossover data of DNA can also be collapsed into a unique function of a scaling variable $z = k(1 - T_\theta/T) \sqrt{M}$. This confirms the two parameter theory hypothesis for DNA, that the static and dynamic properties of DNA in good solvents can be uniquely determined from just two parameters: Radius of gyration at T_θ (R_g^θ) and the solvent quality z . The scaling functions also agree within experimental error with the functions for synthetic polymers and model chains in good solvents obtained using molecular simulations.

The concentration dependence of the zero shear rate viscosity of semidilute solutions of unentangled DNA molecules, across a range of molecular weights, is shown to obey the power

law scaling predicted by blob theory at the θ -temperature. In the crossover region between the θ -temperature and very good solvents, it is seen that the concentration dependence also obeys universal scaling behaviour which can be described by the blob scaling law, but with an effective exponent ν_{eff} that depends on the solvent quality in place of the Flory exponent ν .

The results obtained here demonstrate that it is essential to represent observations in terms of the solvent quality variable z in order to properly understand and characterise the concentration and temperature dependent dynamics of semidilute polymer solutions.

ACKNOWLEDGMENTS

We are grateful to Douglas E. Smith and his group in University of California (San Diego, USA) for preparing the majority of the special DNA fragments and to Brad Olsen, MIT (Cambridge, USA) for the stab cultures containing them. We thank Santosh Noronha and his group (IIT Bombay, India) for helpful discussions, laboratory support, and the two plasmids, pBSKS and pHCMC05, used in this work. JRP gratefully acknowledges very helpful discussions with Burkhard Dünweg. We also acknowledge the funding received from DST, DBT, and MHRD and IITB-Monash Research Academy. The Sophisticated Analytical Instrument Facility (SAIF), IIT Bombay is thanked for access to the static light scattering facility.

See supplementary material at [URL to be inserted by AIP] for details of strains and working conditions; procedures for preparation of linear DNA fragments; solvent composition and quantification of DNA samples; procedure for sample preparation for light scattering; methodology for measuring gyration and hydrodynamic radii, and the approach used here for determining second virial coefficients.

Appendix A: Estimation of the persistence length

At the θ -temperature, since a polymer chain obeys Gaussian statistics, the persistence length P is related to the radius of gyration R_g^θ and the contour length L , through the relation $P = 3(R_g^\theta)^2/L$. In the asymptotic limit $(R_g/L) \ll 1$, this relationship is also valid for a worm-like chain. The persistence lengths evaluated using this expression, at the θ -temperature, from known values of R_g^θ and L , are shown in Figure 20. It is evident from the figure that the persistence length of DNA at a salt concentration of 0.5 M (Na^+) is constant across all the molecular weights, with a mean value

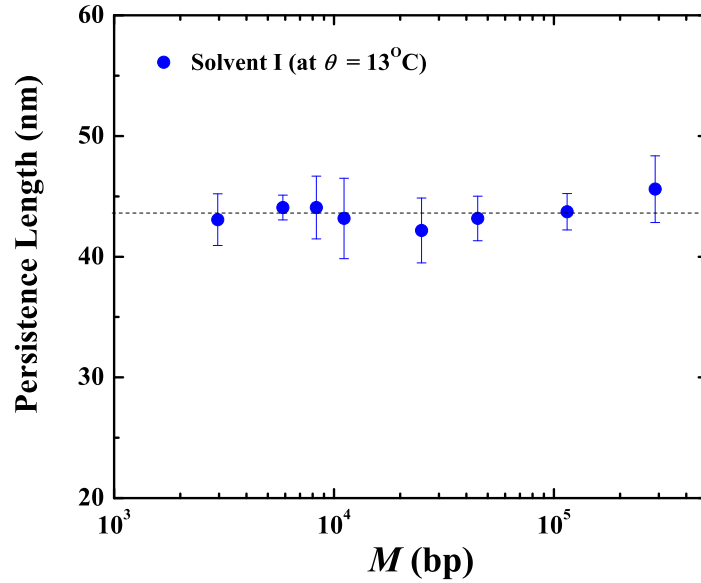


FIG. 20. Molecular weight independence of DNA persistence length.

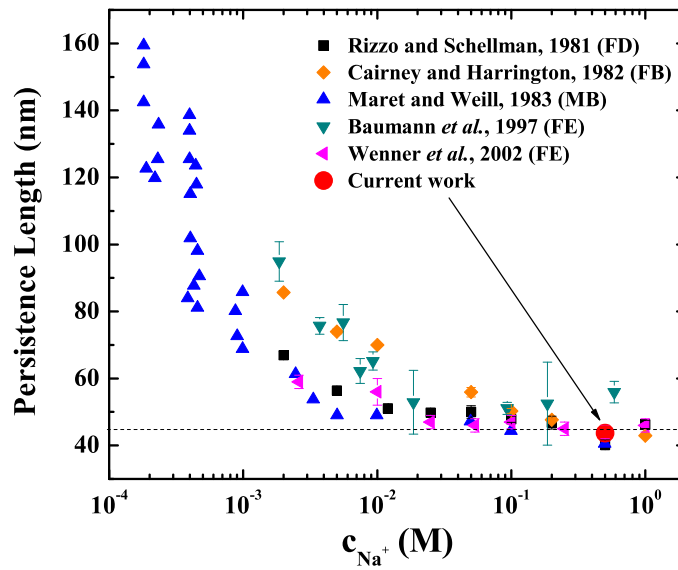


FIG. 21. Dependence of DNA persistence length on salt concentration, collated from data reported previously. The DNA molecular weights used in all these studies range from 3–300 kbp. The mean persistence length for all the molecular weights shown in Figure 20 is denoted here by the opaque red circle. Abbreviations: ‘FD’ - Flow Dichroism, ‘FB’ - Flow Birefringence, ‘MB’ - Magnetic Birefringence, ‘FE’ - Force Extension using optical tweezers.

that is approximately 44 nm.

The effects of salt concentration on the persistence length of DNA has been studied earlier through a variety of techniques such as Flow Dichroism [Rizzo and Schellman, 1981], Flow Birefringence [Cairney and Harrington, 1982], Magnetic Birefringence [Maret and Weill, 1983] and force-extension experiments using optical tweezers [Baumann *et al.*, 1997; Wenner *et al.*, 2002]. Data from a number of these studies has been collated in Figure 21, with the mean value measured in the present study included. Clearly, the persistence length in all the earlier studies appears to reach an approximately constant value of 45-50 nm for salt concentrations > 0.1 M, suggesting that the charges have been fully screened in this concentration regime. Both the value of the persistence length in the high salt limit, and the threshold concentration for charge screening obtained in this work are consistent with earlier observations.

Some early studies of the ionic dependence of DNA persistence length Borochoy *et al.* [1981]; Kam *et al.* [1981]; Sobel and Harpst [1991], investigated via light scattering, have shown a strong dependence of persistence length on salt concentration even up to 4 M. Notably, these measurements were not at the θ -temperature, and consequently, required both an estimation of the solvent quality, and a correction to account for excluded volume effects. The excluded volume corrections applied in the original papers were modified in subsequent studies Hagerman [1988]; Manning [1981]; Schurr and Allison [1981]. These aspects might explain the differences observed from the present study, where both diffusivity and persistence length measurements suggest that charge screening is complete above 10 mM NaCl.

Appendix B: Thermal blobs and measurements in poor solvents

The focus of the experimental measurements in the dilute limit reported in the present paper is twofold: (i) determining the θ -temperature, and (ii) describing the θ to good solvent crossover behaviour of a solution of double-stranded DNA. The analysis of molecular weight scaling under poor solvent conditions has been carried out essentially only in order to locate the θ -temperature. As is well known, the experimental observation of single chains in poor solvents is extremely difficult because of the problem of aggregation due to interchain attraction. Nevertheless, in this section we show that a careful analysis of the data displayed in Figure 3, in the light of the blob picture, enables us to discuss the reliability of the measurements that have been carried out here under poor solvent conditions.

According to the blob picture of dilute polymer solutions, a polymer chain in a good or poor solvent can be considered to be a sequence of thermal blobs, where the thermal blob denotes the length scale at which excluded volume interactions become of order $k_B T$ [Rubinstein and Colby, 2003]. Under good solvent conditions, the blobs obeying self-avoiding-walk statistics, while they are space filling in poor solvents. As a result, the mean size R of a polymer chain is given by [Rubinstein and Colby, 2003],

$$R = R_{\text{blob}}(T) \left(\frac{N_k}{N_{\text{blob}}(T)} \right)^\nu \quad (\text{B1})$$

where, N_k is the number of Kuhn-steps in a chain, N_{blob} is the number of Kuhn-steps in a thermal blob, and R_{blob} is the mean size of a thermal blob. The Flory exponent ν is ≈ 0.59 in a good solvent, and $1/3$ in a poor solvent. The size of the thermal blob is a function of temperature. For instance, under athermal solvent conditions, the entire chain obeys self avoiding walk statistics, so the blob size is equal to the size of a single Kuhn-step. On the other hand, for temperatures approaching the θ -temperature, the blob size grows to engulf the entire chain. From the definitions of Π_H and Π_g (see Eqs. (4)), it is clear that on length scales smaller than the blob length scale both these quantities must remain constant. On the other hand, Eq. (B1) suggests that on length scales large compared to the blob length scale, Π_H and Π_g must scale as $M^{0.09}$ in good solvents, and $M^{-1/6}$ in poor solvents. Figure 22 re-examines the $\log \Pi_H$ versus $\log M$ data for the solvent used in this study in the light of these arguments. It is clear that after an initial regime of constant values, there is a crossover to the expected scaling laws in both the good and poor solvent regimes. The crossover from one scaling regime to the next begins approximately at the blob length scale, an estimate of which can be made as follows.

The requirement that the energy of excluded volume interactions within a thermal blob are of order $k_B T$ leads to the following expressions for N_{blob} and R_{blob} [Rubinstein and Colby, 2003],

$$N_{\text{blob}}(T) = \frac{b_k^6}{v(T)^2} \quad (\text{B2})$$

$$R_{\text{blob}}(T) = \frac{b_k^4}{|v(T)|} \quad (\text{B3})$$

where, b_k is the length of a Kuhn-step, and $v(T)$ is the excluded volume at temperature T . The

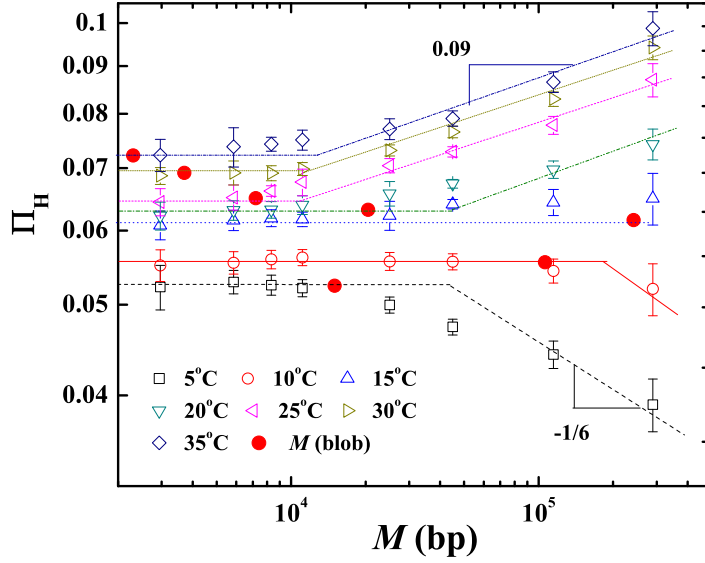


FIG. 22. Different scaling regimes for the scaled variable Π_H as a function of molecular weight M . The filled red circles correspond to the molecular weight M_{blob} of the chain segment within a thermal blob.

excluded volume can be shown to be related to the temperature through the relation,

$$v(T) = \begin{cases} v_0 \left(1 - \frac{T_\theta}{T}\right) & \text{for good solvents,} \\ -v_0 \left(1 - \frac{T}{T_\theta}\right) & \text{for poor solvents.} \end{cases} \quad (\text{B4})$$

where, v_0 is a chemistry dependent constant. These expressions are consistent with the expectation that $v \rightarrow v_0$ in an athermal solvent ($T \rightarrow \infty$), and $v \rightarrow -v_0$ in a non-solvent ($T \rightarrow 0$) [Rubinstein and Colby, 2003]. Since measurements of the mean size (via R_g and R_H) have been carried out here at various temperatures, and we have estimated both T_θ and b_k , it is possible to calculate $v(T)$ in both good and poor solvents using Eqs. (B1) to (B3). As a result the size of a thermal blob as a function of temperature can also be estimated.

The equations that govern the dimensionless excluded volume parameter v_0/b_k^3 and the molecular weight M_{blob} of a chain segment within a thermal blob, in good and poor solvents, are tabulated in Table I, when the hydrodynamic radius R_H is used as a measure of chain size. Here, m_k is the molar mass of a Kuhn-step, and the universal amplitude ratio U_R has been

solvent quality	good	poor
$\frac{v_0}{b_k^3}$ (for $M > M_{\text{blob}}$)	$\left[\frac{a \Pi_H (U_R U_{RD}) m_k^\nu}{b_k} \right]^{\frac{1}{2\nu-1}} \frac{1}{M^{\frac{1}{2}} \left(1 - \frac{T_\theta}{T} \right)}$	$\left[\frac{a \Pi_H (U_R U_{RD})}{b_k} \right]^{-3} \frac{1}{m_k M^{\frac{1}{2}} \left(1 - \frac{T}{T_\theta} \right)}$
$M_{\text{blob}}(T)$	$\frac{m_k b_k^6}{v_0^2 \left(1 - \frac{T_\theta}{T} \right)^2}$	$\frac{m_k b_k^6}{v_0^2 \left(1 - \frac{T}{T_\theta} \right)^2}$

TABLE I. Equations for the dimensionless excluded volume parameter v_0/b_k^3 , and the molecular weight of the chain segment within a thermal blob M_{blob} , in good and poor solvents. Here, m_k is the molar mass of a Kuhn-step, and U_R and U_{RD} are universal amplitude ratios, such that $R = U_R R_g$, and $R_g = U_{RD} R_H$.

used to relate the mean size R to R_g ($R = U_R R_g$), while the universal ratio U_{RD} relates R_g to R_H ($R_g = U_{RD} R_H$). The values of these ratios are known analytically for the case of Gaussian chains and Zimm hydrodynamics under θ -conditions [Doi and Edwards, 1986], and numerically in the case of good solvents [Kumar and Prakash, 2003] and fluctuating hydrodynamic interactions [Sunthar and Prakash, 2006].

Using the known values of a , Π_H , b_k , m_k , U_{RD} , U_R in the appropriate equations in Table I, we find that for sufficiently high molecular weights, $v_0/b_k^3 \approx 4.7 \pm 0.5$ in *both* good and poor solvents. This is significant since an inaccurate measurement of mean size in a poor solvent (as a consequence of, for instance, chain aggregation), would result in different values of v_0/b_k^3 in good and poor solvents. Further evidence regarding the reliability of poor solvent measurements can be obtained by calculating $M_{\text{blob}}(T)$ in good and poor solvents.

Figure 23 displays the variation of M_{blob} with respect to the temperature difference $T - T_\theta$, calculated using the equations given in Table I. The figure graphically demonstrates the temperature dependence of the blob size, and confirms that essentially the blob size is the same in either a good or poor solvent when the temperature is equidistant from the θ -temperature. The symbols in Fig. 23 denote values of M_{blob} , evaluated at the temperatures at which experimental measurements have been made. These values have been represented by the filled red circles in Fig. 22. As can be seen from Fig. 22, the magnitude of M_{blob} is roughly consistent with the location of the crossover from the scaling regime within a blob, to the scaling regime that holds at length scales larger than the blob, in both good and poor solvents. The two scaling regimes, at 25°C, are illustrated explicitly in Fig. 24.

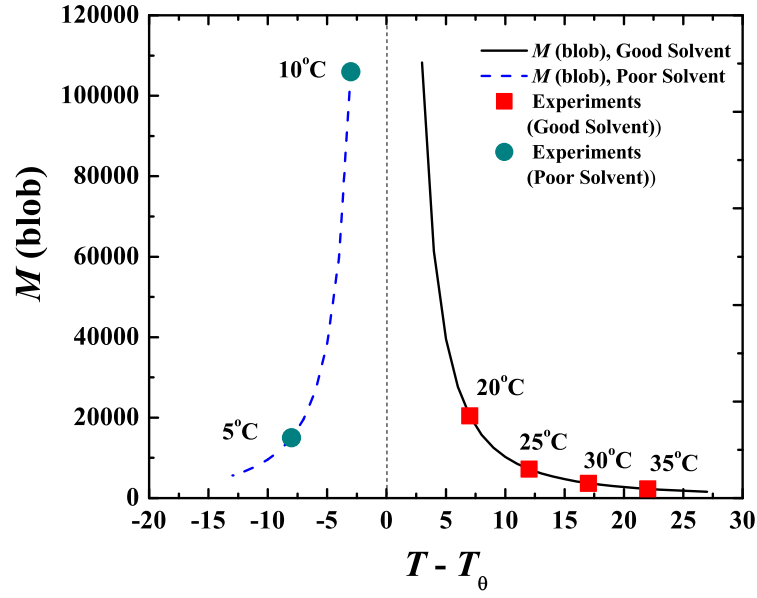


FIG. 23. Variation of the molecular weight of the chain segment within a thermal blob with respect to temperature, on either side of the θ -temperature (see Table I for the equations governing M_{blob}). The symbols denote values at temperatures at which experimental measurements have been made.

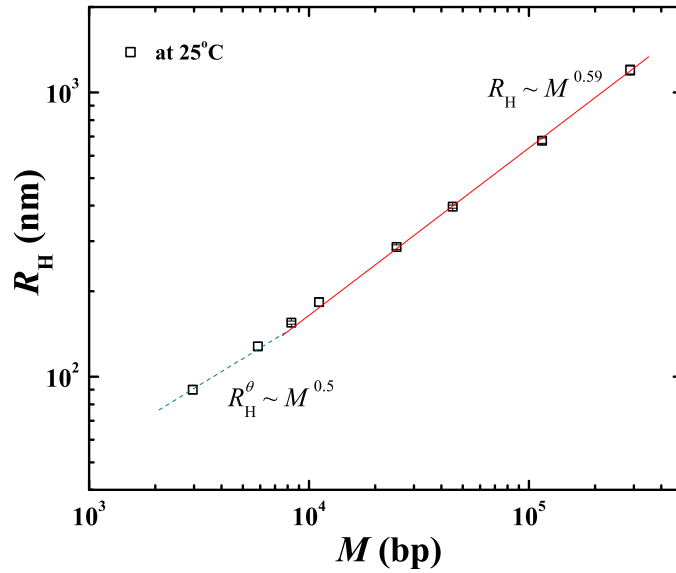


FIG. 24. The variation of hydrodynamic radius (R_H) with molecular weight (in bp) at 25°C.

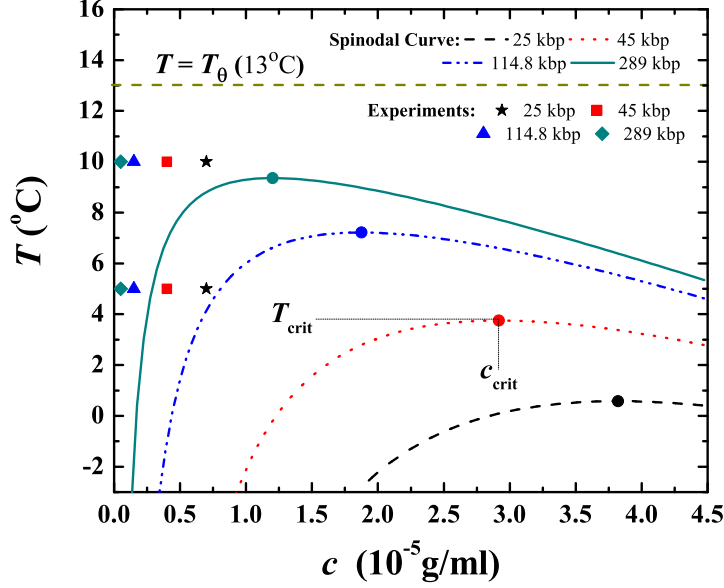


FIG. 25. Spinodal curves and critical temperatures and concentrations (filled circles) predicted by Flory-Huggins mean-field theory for a range of molecular weights. Values of concentrations and temperatures at which the poor solvent experiments have been conducted are also indicated.

The possibility of phase separation under poor solvent conditions, as polymer-solvent interactions become less favourable, is the primary reason for the difficulty of accurately measuring the size scaling of single chains. An approximate estimate of the thermodynamic driving force for phase separation can be obtained with the help of Flory-Huggins mean field theory. Since the Flory-Huggins χ parameter is related to the excluded volume parameter through the relation [Rubinstein and Colby, 2003] $\chi = \frac{1}{2} \left(1 - \frac{v_0}{b_k^3} \right)$, and we have estimated the value of v_0/b_k^3 in both solvents, the phase diagram predicted by Flory-Huggins theory for dilute DNA solutions considered here can be obtained. It is appropriate to note that we are not interested in accurately mapping out the phase diagram for DNA solutions with the help of Flory-Huggins theory. This has already been studied in great detail, using sophisticated versions of mean-field theory, starting with the pioneering work of Post and Zimm [1982], and the problem of DNA condensation is an active field of research [Teif and Bohinc, 2011; Yoshikawa *et al.*, 1996, 2011]. Our primary interest is to obtain an approximate estimate of the location of the current experimental measurements relative to the unstable two-phase region (whose boundary is determined by the spinodal

curve), since phase separation can occur spontaneously within this region. Figure 25 displays the spinodal curves for the 25 to 289 kbp molecular weight samples, predicted by Flory-Huggins theory. Details of how these curves can be obtained are given, for instance, in Rubinstein and Colby [2003]. Also indicated on each curve are the critical concentration and temperature. It is clear by considering the location of the symbols denoting the concentration-temperature coordinates of the poor solvent experiments, that for each molecular weight, they are located outside the unstable two-phase region, lending some justification to the reliability of the present poor solvent measurements. It is appropriate to note here that mean-field theories do not accurately predict the shape of the binodal curve, and in general concentration fluctuations tend to make the curve wider close to the critical point [Rubinstein and Colby, 2003]. Interestingly, even for the 289 kbp sample, that has a very large molecular weight ($\approx 1.9 \times 10^8$ Dalton), there is still a considerable gap between the critical and θ -temperatures ($\approx 4^\circ\text{C}$). The reason for this is because the stiffness of double-stranded DNA leads to a relatively small number of Kuhn-steps (1120) even at this large value of molecular weight, and the value of the critical temperature predicted by Flory-Huggins theory depends on the number of Kuhn-steps in a chain rather than the molecular weight.

REFERENCES

- Ahirwal, D., S. Pan, Duc At Nguyen, P. Sunthar, T. Sridhar and J. R. Prakash, “Swelling of intrinsic viscosity radius for dilute polymer solutions: DNA rheology and Brownian dynamics simulations,” Under preparation (2012).
- Ahlrichs, P., R. Everaers and B. Duenweg, “Screening of hydrodynamic interactions in semidilute polymer solutions: A computer simulation study,” *Phys.Rev. E* **64**, 040501 (2001).
- Babcock, H. P., R. E. Teixeira, J. S. Hur, E. S. G. Shaqfeh and S. Chu, “Visualization of molecular fluctuations near the critical point of the coil-stretch transition in polymer elongation,” *Macromolecules* **36**, 4544–4548 (2003).
- Barrat, J.-L. and J.-F. Joanny, “Theory of polyelectrolyte solutions,” *Adv. Chem. Phys.* **94** (XCIV), 1–66 (1996).
- Barrett, A. J., M. Mansfield and B. C. Benesch, “Numerical study of self-avoiding walks on lattices and in the continuum,” *Macromolecules* **24**, 1615–1621 (1991).
- Baumann, C. G., S. B. Smith, V. A. Bloomfield and C. Bustamante, “Ionic effects on the elasticity of single dna molecules,” *Proc. Natl. Acad. Sci. U. S. A.* **94**, 6185–6190 (1997).

Borochoy, N., H. Eisenberg and Z. Kam, “Dependence of dna conformation on the concentration of salt,” *Biopolymers* **20**, 231–235 (1981).

Bustamante, C., J. F. Marko, E. D. Siggia and S. Smith, “Entropic elasticity of DNA,” *Science* **265**, 1599–1600 (1994).

Cairney, K. L. and R. E. Harrington, “Flow birefringence of t7 phage dna: dependence on salt concentration,” *Biopolymers* **21**, 923–934 (1982).

Chirico, G., P. Crisafulli and G. Baldini, “Dynamic light scattering of dna: Role of the internal motion,” *Il Nuovo Cimento D* **11**, 745–759 (1989).

de Gennes, P.-G., *Scaling Concepts in Polymer Physics*, Cornell University Press, Ithaca (1979).

Doi, M. and S. F. Edwards, *The Theory of Polymer Dynamics*, Clarendon Press, Oxford, New York (1986).

Domb, C. and A. J. Barrett, “Universality approach to the expansion factor of a polymer chain,” *Polymer* **17**, 179–184 (1976).

Doty, P., B. B. McGill and S. A. Rice, “The properties of sonic fragments of deoxyribose nucleic acid,” *Proc. Natl. Acad. Sci. U. S. A.* **44**, 432–438 (1958).

Fishman, D. M. and G. D. Patterson, “Light scattering studies of supercoiled and nicked dna,” *Biopolymers* **38**, 535–552 (1996).

Fujimoto, B. S., J. M. Miller, N. S. Ribeiro and J. M. Schurr, “Effects of different cations on the hydrodynamic radius of dna,” *Biophys. J.* **67**, 304–308 (1994).

Graessley, W. W., “Polymer chain dimensions and the dependence of viscoelastic properties on concentration, molecular weight and solvent power,” *Polymer* **21**, 258 – 262 (1980).

Grosberg, A. Y. and A. R. Khokhlov, *Statistical physics of macromolecules*, AIP Press, New York (1994).

Hagerman, P. J., “Flexibility of dna,” *Annual review of biophysics and biophysical chemistry* **17**, 265–286 (1988).

Hayward, R. C. and W. W. Graessley, “Excluded volume effects in polymer solutions. 1. dilute solution properties of linear chains in good and theta solvents,” *Macromolecules* **32**, 3502–3509 (1999).

Heo, Y. and R. G. Larson, “The scaling of zero-shear viscosities of semidilute polymer solutions with concentration,” *Journal of Rheology* **49**, 1117–1128 (2005).

Heo, Y. and R. G. Larson, “Universal scaling of linear and nonlinear rheological properties of semidilute and concentrated polymer solutions,” *Macromolecules* **41**, 8903–8915 (2008).

Hodnett, J. L., R. J. Legerski and H. B. Gray Jr., "Dependence upon temperature of corrected sedimentation coefficients measured in a beckman analytical ultracentrifuge," *Anal. Biochem.* **75**, 522–537 (1976).

Huang, C.-C., R. G. Winkler, G. Sutmann and G. Gompper, "Semidilute polymer solutions at equilibrium and under shear flow," *Macromolecules* **43**, 10107–10116 (2010).

Hur, J. S., E. S. G. Shaqfeh, H. P. Babcock, D. E. Smith and S. Chu, "Dynamics of dilute and semidilute dna solutions in the start-up of shear flow," *J. Rheol.* **45**, 421–450 (2001).

Kam, Z., N. Borochoy and H. Eisenberg, "Dependence of laser light scattering of dna on nacl concentration," *Biopolymers* **20**, 2671–2690 (1981).

Krigbaum, W. R., "Statistical mechanics of dilute polymer solutions. vi. thermodynamic parameters for the system polystyrene-cyclohexane," *J. Am. Chem. Soc.* **76**, 3758–3764 (1954).

Kröger, M., A. Alba-Pérez, M. Laso and H. C. Öttinger, "Variance reduced brownian simulation of a bead-spring chain under steady shear flow considering hydrodynamic interaction effects," *J. Chem. Phys.* **113**, 4767–4773 (2000).

Kumar, K. S. and J. R. Prakash, "Equilibrium swelling and universal ratios in dilute polymer solutions: Exact brownian dynamics simulations for a delta function excluded volume potential," *Macromolecules* **36**, 7842–7856 (2003).

Kumar, K. S. and J. R. Prakash, "Universal consequences of the presence of excluded volume interactions in dilute polymer solutions undergoing shear flow," *J. Chem. Phys.* **121**, 3886–3897 (2004).

Laib, S., R. M. Robertson and D. E. Smith, "Preparation and characterization of a set of linear dna molecules for polymer physics and rheology studies," *Macromolecules* **39**, 4115–4119 (2006).

Langowski, J., "Salt effects on internal motions of superhelical and linear puc8 dna. dynamic light scattering studies," *Biophys. Chem.* **27**, 263–271 (1987).

Leighton, S. B. and I. Rubenstein, "Calibration of molecular weight scales for dna," *J. Mol. Biol.* **46**, 313–328 (1969).

Liu, H., J. Gapinski, L. Skibinska, A. Patkowski and R. Pecora, "Effect of electrostatic interactions on the dynamics of semiflexible monodisperse dna fragments," *J. Chem. Phys.* **113**, 6001–6010 (2000).

Liu, Y., Y. Jun and V. Steinberg, "Concentration dependence of the longest relaxation times of dilute and semi-dilute polymer solutions," *J. Rheol.* **53**, 1069–1085 (2009).

Manning, G., "A procedure for extracting persistence lengths from light-scattering data on inter-

mediate molecular weight dna,” *Biopolymers* **20**, 1751–1755 (1981).

Marathias, V. M., B. Jerkovic, H. Arthanari and P. H. Bolton, “Flexibility and curvature of duplex dna containing mismatched sites as a function of temperature,” *Biochemistry* **39**, 153–160 (2000).

Maret, G. and G. Weill, “Magnetic birefringence study of the electrostatic and intrinsic persistence length of dna,” *Biopolymers* **22**, 2727–2744 (1983).

Marko, J. F. and E. D. Siggia, “Stretching DNA,” *Macromolecules* **28**, 8759–8770 (1995).

Miyaki, Y. and H. Fujita, “Excluded-volume effects in dilute polymer solutions. 11. Tests of the two-parameter theory for radius of gyration and intrinsic viscosity,” *Macromolecules* **14**, 742–746 (1981).

Nayvelt, I., T. Thomas and T. J. Thomas, “Mechanistic differences in dna nanoparticle formation in the presence of oligolysines and poly-l-lysine,” *Biomacromolecules* **8**, 477–484 (2007).

Nicolai, T. and M. Mandel, “Dynamic light scattering by aqueous solutions of low-molar-mass dna fragments in the presence of sodium chloride,” *Macromolecules* **22**, 2348–2356 (1989).

Orofino, T. A. and J. W. Mickey Jr., “Dilute solution properties of linear polystyrene in -solvent media,” *J. Chem. Phys.* **38**, 2512–2520 (1963).

Ottinger, H. C., *Stochastic Processes in Polymeric Fluids*, Springer, Berlin (1996).

Pecora, R., “Dna: A model compound for solution studies of macromolecules,” *Science* **251**, 893–898 (1991).

Post, C. B. and B. H. Zimm, “Theory of DNA condensation: Collapse versus aggregation,” *Biopolymers* **21**, 2123–2137 (1982).

Prakash, J. R., “Rouse chains with excluded volume interactions in steady simple shear flow,” *J. Rheol.* **46**, 1353–1380 (2002).

Rizzo, V. and J. Schellman, “Flow dichroism of t7 dna as a function of salt concentration,” *Biopolymers* **20**, 2143–2163 (1981).

Robertson, R. M., S. Laib and D. E. Smith, “Diffusion of isolated dna molecules: Dependence on length and topology,” *Proc. Natl. Acad. Sci. U. S. A.* **103**, 7310–7314 (2006).

Ross, P. D. and R. L. Scruggs, “Viscosity study of dna. ii. the effect of simple salt concentration on the viscosity of high molecular weight dna and application of viscometry to the study of dna isolated from t4 and t5 bacteriophage mutants,” *Biopolymers - Peptide Science Section* **6**, 1005–1018 (1968).

Rubinstein, M. and R. H. Colby, *Polymer Physics*, Oxford University Press (2003).

Sambrook, J. and D. W. Russell, *Molecular Cloning: A Laboratory Manual (3rd edition)*, Cold

Spring Harbor Laboratory Press, USA (2001).

Schäfer, L., *Excluded Volume Effects in Polymer Solutions*, Springer-Verlag, Berlin (1999).

Schroeder, C. M., H. P. Babcock, E. S. G. Shaqfeh and S. Chu, "Observation of polymer conformation hysteresis in extensional flow," *Science* **301**, 1515–1519 (2003).

Schurr, J. M. and S. A. Allison, "Polyelectrolyte contribution to the persistence length of dna," *Biopolymers* **20**, 251–268 (1981).

Selis, J. and R. Pecora, "Dynamics of a 2311 base pair superhelical dna in dilute and semidilute solutions," *Macromolecules* **28**, 661–673 (1995).

Shultz, A. R. and P. J. Flory, "Phase equilibria in polymer-solvent systems," *J. Am. Chem. Soc.* **74**, 4760–4767 (1952).

Sibileva, M. A., A. N. Veselkov, S. V. Shilov and E. V. Frisman, "Effect of temperature on the conformation of native dna in aqueous solutions of various electrolytes [vliianie temperatury na konformatsiiu molekuly nativno dnk v vodnykh rastvorakh razlichnykh lektrolitov.]," *Molekulyarnaya Biologiya* **21**, 647–653 (1987).

Smith, D. E. and S. Chu, "Response of flexible polymers to a sudden elongational flow," *Science* **281**, 1335–1340 (1998).

Smith, D. E., T. T. Perkins and S. Chu, "Dynamical scaling of DNA diffusion coefficients," *Macromolecules* **29**, 1372–1373 (1996a).

Smith, D. E., T. T. Perkins and S. Chu, "Dynamical scaling of dna diffusion coefficients," *Macromolecules* **29**, 1372–1373 (1996b).

Sobel, E. S. and J. A. Harpst, "Effects of na⁺ on the persistence length and excluded volume of t7 bacteriophage dna," *Biopolymers* **31**, 1559–1564 (1991).

Soda, K. and A. Wada, "Dynamic light-scattering studies on thermal motions of native dnas in solution," *Biophys. Chem.* **20**, 185–200 (1984).

Somani, S., E. S. G. Shaqfeh and J. R. Prakash, "Effect of solvent quality on the coil-stretch transition," *Macromolecules* **43**, 10679–10691 (2010).

Sorlie, S. S. and R. Pecora, "A dynamic light scattering study of four dna restriction fragments," *Macromolecules* **23**, 487–497 (1990).

Stoltz, C., J. J. de Pablo and M. D. Graham, "Concentration dependence of shear and extensional rheology of polymer simulations: Brownian dynamics simulations," *J.Rheol.* **502**, 137 (2006).

Sunthar, P., D. A. Nguyen, R. Dubbelboer, J. R. Prakash and T. Sridhar, "Measurement and prediction of the elongational stress growth in a dilute solution of DNA molecules," *Macromolecules*

38, 10200–10209 (2005).

Sunthar, P. and J. R. Prakash, “Parameter free prediction of DNA conformations in elongational flow by successive fine graining,” *Macromolecules* **38**, 617–640 (2005).

Sunthar, P. and J. R. Prakash, “Dynamic scaling in dilute polymer solutions: The importance of dynamic correlations,” *Europhys. Lett.* **75**, 77–83 (2006).

Teif, V. B. and K. Bohinc, “Condensed dna: Condensing the concepts,” *Progress in Biophysics and Molecular Biology* **105**, 208 – 222 (2011).

Tominaga, Y., I. I. Suda, M. Osa, T. Yoshizaki and H. Yamakawa, “Viscosity- and hydrodynamic-radius expansion factors of oligo- and poly(a-methylstyrene)s in dilute solution,” *Macromolecules* **35**, 1381–1388 (2002).

Valle, F., M. Favre, P. De Los Rios, A. Rosa and G. Dietler, “Scaling exponents and probability distributions of dna end-to-end distance,” *Phys. Rev. Lett.* **95**, 1–4 (2005).

Wenner, J. R., M. C. Williams, I. Rouzina and V. A. Bloomfield, “Salt dependence of the elasticity and overstretching transition of single dna molecules,” *Biophys. J.* **82**, 3160–3169 (2002).

Yamakawa, H., *Modern Theory of Polymer Solutions*, Kyoto University (formerly by Harper and Row), Kyoto, electronic edn. (2001).

Yoshikawa, K., M. Takahashi, V. Vasilevskaya and A. Khokhlov, “Large Discrete Transition in a Single DNA Molecule Appears Continuous in the Ensemble,” *Phys. Rev. Lett.* **76**, 3029–3031 (1996).

Yoshikawa, Y., Y. Suzuki, K. Yamada, W. Fukuda, K. Yoshikawa, K. Takeyasu and T. Imanaka, “Critical behavior of megabase-size dna toward the transition into a compact state,” *J. Chem. Phys.* **135**, 225101 (2011).

Zimm, B. H., “Dynamics of polymer molecules in dilute solution: Viscoelasticity, flow birefringence and dielectric loss,” *J. Chem. Phys.* **24**, 269–281 (1956).

Supplementary material for:

Universal solvent quality crossover of the zero shear rate viscosity of semidilute DNA solutions

Sharadwata Pan,^{1,2,3} Duc At Nguyen,³ P. Sunthar,^{2,1} T. Sridhar,^{3,1} and J. Ravi Prakash^{3,1, a)}

¹⁾*IITB-Monash Research Academy, Indian Institute of Technology Bombay, Powai, Mumbai - 400076, India*

²⁾*Department of Chemical Engineering, Indian Institute of Technology Bombay, Powai, Mumbai - 400076, India*

³⁾*Department of Chemical Engineering, Monash University, Melbourne, VIC 3800, Australia*

(Dated: 8 November 2019)

^{a)}Corresponding author: ravi.jagadeeshan@monash.edu

I. DETAILS OF STRAINS, WORKING CONDITIONS AND PROCEDURES FOR PREPARING LINEAR DNA FRAGMENTS.

Recently, a range of special DNA constructs, from 3 – 300 kbp, have been genetically engineered into bacterial strains of *E. coli* [Laib *et al.*, 2006], which can be selectively extracted for rheological studies. Primarily they fall into three categories: plasmids, fosmids and Bacterial Artificial Chromosomes (BAC). Altogether six samples (two plasmids, two fosmids and two BACs), which were originally prepared elsewhere [Laib *et al.*, 2006] were procured from Dr. Brad Olsen, California Institute of Technology, USA. Throughout the work, the nomenclature of all the three types of DNA samples has been used as in the originally published work [Laib *et al.*, 2006]. In addition, two special bacterial strains containing the plasmids: pBSKS (2.7 kbp) and pHCMC05 (8.3 kbp) were provided by Dr. S. Noronha, Dept. of Chemical Engineering, IIT Bombay (India). The details about size, growth conditions of bacteria and single cutters of the DNA samples are mentioned in Table I. After procurement of samples (in the form of agar stab cultures of *E. coli*), glycerol freeze stocks were made using 50% glycerol and stored at -80°C. The cultures can be stored in this way for several years and can be used at any time to produce DNA samples [Laib *et al.*, 2006].

Standard procedures [Laib *et al.*, 2006; Sambrook and Russell, 2001] involving alkaline lysis (mediated by NaOH) were adopted for extraction, linearization and purification of plasmids, fosmids and BAC from the cultures. For high copy number plasmids, no inducer was added. For low (fosmids) and very low (BACs) copy number samples, L-arabinose was added as inducer. From each freeze stock, 15µl of ice was scrapped and transferred to 40 ml LB medium with proper antibiotic (as mentioned in Table I) and incubated overnight (16 – 18 hours) at 37°C with vigorous shaking (200 – 250 rpm). The overnight grown culture was poured into microcentrifuge tubes and cells were harvested by centrifugation. The bacterial pellet (obtained above) was resuspended in 100µl of ice-cold Solution I (4°C) followed by 200µl of freshly prepared Solution II and 150µl of ice-cold Solution III [Sambrook and Russell, 2001]. The tubes were stored on ice for 3–5 minutes and centrifuged. The supernatant was transferred to a fresh tube. The precipitate (containing mainly the cell debris and genomic DNA) was discarded. RNase was added (at 10 µg/ml) to the tube and incubated at 37°C for 20 minutes. Equal volume of Phenol-Chloroform-Isoamyl Alcohol (25:24:1) mixture was added and mixed well by vortexing. After centrifugation, supernatant was transferred to a fresh tube. Equal volume of Chloroform was added and centrifuged. The super-

TABLE I. DNA Fragments. Here 'LB' stands for Luria Bertini broth, 'Ant^R' refers to Antibiotic resistance, 'Amp.' refers to Ampicillin, 'CAM' refers to Chloramphenicol, 'Kan' refers to Kanamycin, all the cultures were incubated overnight at 37°C with vigorous shaking (200–250 rpm). L-arabinose (inducer) was used at a concentration of 0.01g per 100 ml (stock concentration: 5g in 100ml). Stock concentrations for preparations of Ampicillin, Chloramphenicol and Kanamycin were 100 mg/ml, 25 mg/ml and 100 mg/ml respectively. The working concentrations for Amp., CAM and Kan are 100 µg/ml, 12.5µg/ml and 100µg/ml respectively. Growth conditions for all the plasmids are same (LB + Amp.) except pHCMC05 (LB + Amp. + CAM). For both the fosmids, growth conditions are identical (LB + CAM + L-arabinose). For both the BACs, growth conditions are same (LB + CAM + Kan + L-arabinose).

Type	Name	Size (kb) /(Notation)	Ant ^R	1 Cutter
Plasmid	pBSKS(+)	2.9 / F2.9	Amp.	BamHI
	pYES2	5.9 / F5.9	Amp.	BamHI
	pHCMC05	8.3 / F8.3	Amp. + CAM	BamHI
	pPIC9K<TRL5>	11.1 / F11.1	Amp.	
Fosmid	pCC1FOS-25	25 / F25	CAM	ApaI
	pCC1FOS-45	45 / F45	CAM	ApaI
BAC	CTD-2342K16	114.8 / F114.8	CAM + Kan	MluI
	CTD-2657L24	289 / F289	CAM + Kan	MluI

nant was transferred to a fresh tube. Two volumes of chilled 100% ethanol (at 4°C) was added at room temperature kept for 7–8 hours at -20°C. The tube was then centrifuged and the supernatant removed by gentle aspiration. The tube was kept in an inverted position in a paper towel to allow all of the fluid to drain away. Following this, 1 ml of 70% ethanol was added to the tube and centrifuged. When all of the ethanol was evaporated, the resulting DNA pellet was dissolved in 50µl of Milli-Q grade water and stored at -20°C.

To linearize the extracted DNA fragments, 39µl of water was added to a 1.7 ml microcentrifuge tube, followed by 10µl of corresponding 10X Assay Buffer (working concentration is 1X) and 50µl of DNA solution (purified DNA stored at 4°C). 1 µl of appropriate enzyme was added. A thumb rule is 0.5 - 1 U enzyme for 1 mg DNA [Sambrook and Russell, 2001]. The samples were mixed well with micropipette (wide bore tips) for several times. The reaction mix (100µl) was

TABLE II. Composition of the solvent used in the study.

10 mM Tris
1 mM EDTA
0.5 M NaCl
Water

incubated at 37°C for three hours. After restriction digestion / linearization, it is necessary to remove the enzymes / other reagents present in the reaction mix so that they do not interfere with the downstream application/s like light scattering studies, rheometry etc. For this normal phenol-chloroform extraction followed by ethanol precipitation of DNA was carried out as described elsewhere [Sambrook and Russell, 2001].

II. SOLVENT COMPOSITION

The solvent used in this study (see Table II) is primarily the widely used Tris-EDTA buffer, supplemented with 0.5 M NaCl. The measured viscosity of the solvent at 20°C is 1.01 mPa-s.

III. QUANTIFICATION OF DNA SAMPLES

After the DNA samples were extracted and purified, their purity were determined using the Nano-Photometer (UV-VIS Spectrophotometer, IMPLÉN, Germany). Optical Density (O.D.) readings were taken at three different wavelengths: 260 nm, 280 nm and 230 nm. The ratio of absorbance at 260 nm to that of 280 nm gives a rough indication of DNA purity [Sambrook and Russell, 2001]. The concentrations were calculated from absorbance reading at 260 nm (DNA shows absorption peak at 260 nm) by Beer-Lambert's Law [Sambrook and Russell, 2001] and also by agarose gel electrophoresis through a serial dilution of DNA samples as suggested elsewhere [Laib *et al.*, 2006]. All the linear DNA samples demonstrated A_{260}/A_{280} ratio of 1.8 and above. This indicates good purity for DNA samples, though it is largely an assumption [Laib *et al.*, 2006] and A_{260}/A_{230} ratio from 2.0 to 2.2 (absence of organic reagents like phenol, chloroform etc) [Laib *et al.*, 2006]. The low molecular weight linear DNA fragments (plasmids) were quantified through agarose gel electrophoresis with a known standard 1 kbp DNA marker (Fermentas).

TABLE III. c^* values (in $\mu\text{g/ml}$) for different DNA fragments used in this study at different temperatures.

Size (kbp)	15°C	20°C	25°C	30°C	35°C
2.9	353	323	295	241	210
5.9	244	231	210	154	141
8.3	198	187	163	124	104
11.1	172	152	129	103	84
25	110	90	75	60	53
45	68	51	39	34	28
114.8	31	22	15	12	10
289	16	8	5	4	3

For low copy number fragments (fosmids) and very low copy number samples (BACs), it was confirmed that the samples were not sheared during extraction by running a very low concentration agarose gel for extended period at low voltage. A loss of 25% – 50% was observed in the amount of DNA samples after the linearization procedure. This is attributed to purification steps by phenol-chloroform extraction [Sambrook and Russell, 2001].

IV. SAMPLE PREPARATION FOR LIGHT SCATTERING

All the linear DNA fragments were dissolved individually in the solvent and were characterized by dynamic light scattering (DLS) for the hydrodynamic radius, R_H and by static light scattering (SLS) for the radius of gyration, R_g . For both dynamic and static light scattering, an extensive sample preparation method was followed to ensure repeatability. The methodology of sample preparation was modified from earlier studies [Lewis *et al.*, 1985; Selis and Pecora, 1995; Sorlie and Pecora, 1990] and was repeated before each measurement. The cuvette was washed with ethanol (0.5 ml) for 5 times and kept for 15 minutes inside laminar air flow. It was followed by wash with milliQ grade water for 10 – 15 minutes continuously. In the meantime, the solvents were filtered with 0.45μ membrane-filter (PALL Corp., USA) with 2 different membranes consecutively. After filtration, DNA was added to make final concentration of $c/c^* = 0.1$ (for DLS) and $c/c^* = 0.05 - 0.1$ (for SLS). The c^* values for different DNA fragments used in this study at different temperatures are summarized in Table III.

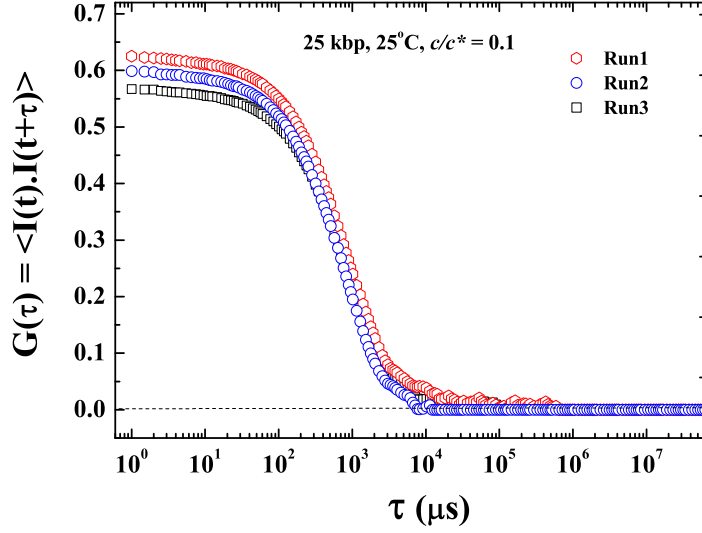


FIG. 1. Intensity autocorrelation spectra for 25 kbp DNA at 25°C and $c/c^* = 0.1$.

V. CHARACTERIZATION OF LINEAR DNA SAMPLES

Dynamic Light Scattering was used for measuring the hydrodynamic radii of all the molecular weights at different temperatures: 5°C, 10°C, 15°C, 20°C, 25°C, 30°C and 35°C. Static Light Scattering was used for measuring the radii of gyration of all the molecular weights at different temperatures: 15°C, 20°C, 25°C, 30°C and 35°C. Static Light Scattering was also used to find out the second virial coefficients at different temperatures: 11.2°C, 13°C, 14°C, 15°C and 20°C.

VI. DYNAMIC LIGHT SCATTERING: TAKING MEASUREMENTS

The dynamic size characterization of dilute DNA solutions was done using a Zetasizer Nano ZS (ZEN3600, MALVERN, U.K.) particle size analyzer with temperature control fitted with a 633 nm He-Ne laser using back-scattering detection. This instrument uses dynamic light scattering (or quasi-elastic light scattering / photon correlation spectroscopy) to measure the diffusion coefficient which is then converted to an average hydrodynamic size of particles in solution using the Stokes-Einstein equation. A Standard Operating Procedure (SOP) was created using the Dispersion Technology Software (DTS 5.00, MALVERN, U.K.) to achieve the desired outcome (R_H) without manual intervention. Scattering of the DNA solutions was measured at a fixed 173° scattering angle (this enables measurements even at high sample concentrations and the effect of

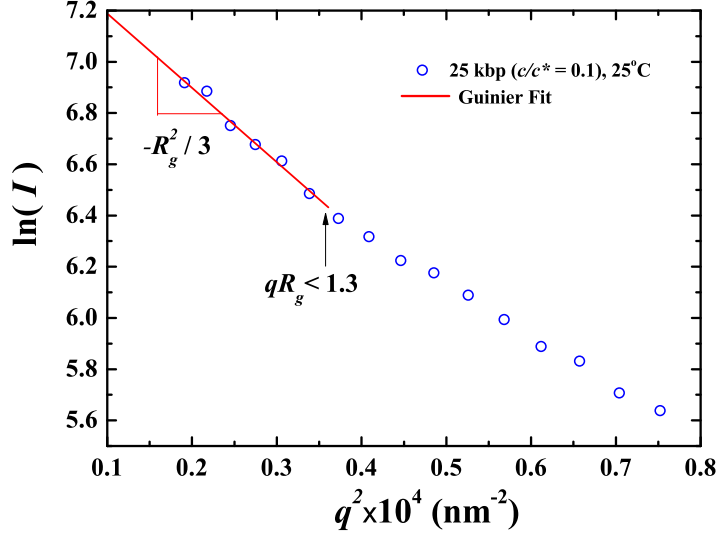


FIG. 2. Application of the Guinier approximation. Intensity as a function of scattering wave vector, measured for 25 kbp DNA at 25°C and $c/c^* = 0.1$.

dust is greatly reduced). The temperature range investigated was from 5 to 35°C . A typical example of measured intensity autocorrelation spectra for 25 kbp DNA at 25°C and $c/c^* = 0.1$ is shown in Figure 1. Note that, $G(\tau) = \langle I(t)I(t + \tau) \rangle$, where I is the intensity of scattered light, and τ is the time difference of the correlator. The Zetasizer Nano ZS has the ability to measure a wide size range (0.6–6000 nm in diameter). In this paper, we have reported sizes roughly in the range 140–2800 nm in diameter, which is within the size range of the instrument. Readings were taken in three temperature scans (a sequence of High-Low, Low-High, and High-Low temperature settings); with 5 readings at each temperature. The mean of 15 readings was taken as final data point at each temperature for each DNA fragment.

Measured values of R_H are reported in Table IV. As expected, the hydrodynamic radius of DNA increases with both temperature and molecular weight. The values of R_H^θ obtained by linear interpolation are indicated in italics.

VII. STATIC LIGHT SCATTERING: TAKING MEASUREMENTS

The static light scattering (SLS) measurements were obtained from a BI-200SM Goniometer (Brookhaven Instruments Corporation, USA) using BI-SLSW Static Light Scattering Software.

TABLE IV. Hydrodynamic Radius (R_H) of linear DNA at different temperatures. Each data point corresponds to the intensity peaks from DLS measurements. The mean of 15 readings was taken as final data point at each temperature for each DNA fragment. The values of R_H^θ obtained by linear interpolation are indicated in italics.

Sequence length	2.9 kbp	5.9 kbp	8.3 kbp	11.1 kbp
Temperature	R_H (in nm)	R_H (in nm)	R_H (in nm)	R_H (in nm)
5°C	73±4	104±3	123±3	141±3
10°C	77±3	109±3	131±3	152±3
13°C	79±2	<i>115±4</i>	<i>137±3</i>	<i>157±3</i>
15°C	85±3	121±3	145±3	167±3
20°C	87±3	124±3	148±3	173±4
25°C	90±3	131±5	155±2	183±6
30°C	96±2	136±4	162±3	189±3
35°C	101±4	145±7	174±3	203±5

Sequence length	25 kbp	45 kbp	114.8 kbp	289 kbp
Temperature	R_H (in nm)	R_H (in nm)	R_H (in nm)	R_H (in nm)
5°C	203±4	258±5	385±13	540±35
10°C	226±5	303±6	473±14	718±46
13°C	239±7	<i>315±9</i>	<i>503±13</i>	<i>789±40</i>
15°C	258±3	349±4	560±18	897±57
20°C	267±8	367±4	607±13	1025±39
25°C	286±5	397±5	677±15	1201±49
30°C	297±4	417±6	722±13	1300±38
35°C	313±8	431±8	753±19	1363±57

A separate temperature control system (PolySc, USA) was arranged. For R_g measurements, the readings for each molecular weight were taken at different angles at different temperatures. The Guinier approximation for calculating R_g was employed. The angle range was selected based on sample concentration. A typical example of the application of the Guinier approximation for 25

TABLE V. Radius of gyration (R_g) of linear DNA fragments at different temperatures. Each data corresponds to an average of 10 measurements performed in two temperature scans. The R_g values at $T_\theta = 13^\circ\text{C}$ have been estimated by linear extrapolation of data points, and indicated in italics.

Sequence length	2.9 kbp	5.9 kbp	8.3 kbp	11.1 kbp
Temperature	R_g (in nm)	R_g (in nm)	R_g (in nm)	R_g (in nm)
<i>13°C</i>	<i>125±2</i>	<i>174±4</i>	<i>206±5</i>	<i>234±9</i>
15°C	129±2	184±5	221±7	255±6
20°C	133±5	187±8	225±8	266±9
25°C	137±6	193±5	236±4	281±8
30°C	147±3	214±4	258±2	303±7
35°C	154±3	220±5	274±4	324±9

Sequence length	25 kbp	45 kbp	114.8 kbp	289 kbp
Temperature	R_g (in nm)	R_g (in nm)	R_g (in nm)	R_g (in nm)
<i>13°C</i>	<i>342±11</i>	<i>458±10</i>	<i>744±13</i>	<i>1212±37</i>
15°C	389±6	554±15	980±22	1667±46
20°C	415±5	612±14	1098±24	2102±30
25°C	441±5	666±10	1242±23	2426±38
30°C	476±7	696±10	1347±17	2664±43
35°C	495±7	743±21	1415±32	2782±47

kbp DNA at 25°C and $c/c^* = 0.1$ is shown in Figure 2. The temperature range investigated was from $15-35^\circ\text{C}$. Readings were taken in two temperature scans; with 5 repeats at each temperature. The mean of 10 repeats was taken as final data point at each temperature for each DNA fragment. For determining the transition in the second virial coefficient (at the theta temperature), the intensity of scattered light was measured as a function of scattering vector (which is a function of the scattering angle) and DNA concentrations. R_g of the DNA increase with both temperature and molecular weight. This is reported in Table V. The values of R_g^θ obtained by linear extrapolation are indicated in italics.

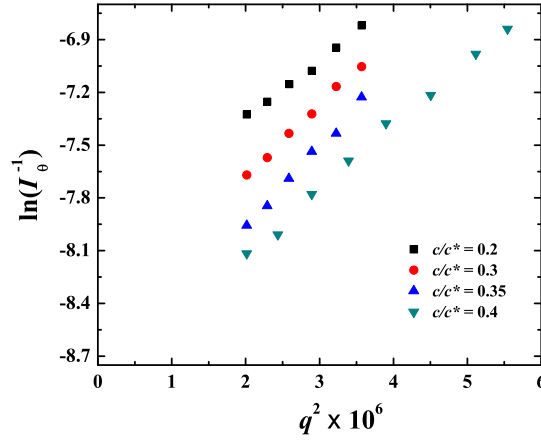


FIG. 3. Variation of reciprocal intensity for 25 kb linear DNA as a function of q^2 (at 20°C). Here, q^2 is a function of the scattering angle. The readings are extrapolated to find the intensity at zero scattering angle, I_o .

VIII. DETERMINATION OF SECOND VIRIAL COEFFICIENTS BY SLS

In this work, a single, linear, medium molecular weight DNA fragment (25 kbp) is taken and the intensity of scattered light, I_θ is determined as a function of scattering vector, q^2 and polymer concentration, c through SLS, at temperatures above and below the estimated θ -point. The readings from a typical plot of reciprocal scattering intensity ($1/I_\theta$) against q^2 (see Figure 3), are extrapolated to find the intensity at zero scattering angle (I_o). Intensity readings are taken at 5 different temperatures between 10 – 20°C. Four different concentrations are used: $c/c^* = 0.2, 0.3, 0.35$ and 0.4 (c^* is the overlap concentration, based on our measured R_g). The second virial coefficients are determined according to a procedure described in Ref. Orofino and Mickey Jr., 1963. The dependence of reduced scattering ratios at zero angle (c/I_o) on the reduced concentration (c/c^*) can be written as [Orofino and Mickey Jr., 1963] :

$$(c/I_o)^{1/2} = (1/M)[1 + A_2(c/c^*) + A_3(c/c^*)^2 + \dots] \quad (1)$$

Here, M is Molecular Weight, A_2 is second virial coefficient and A_3 and subsequent coefficients resemble interaction terms of higher order. From the plots of $(c/I_o)^{1/2}$ against c/c^* (see Figure 4), slopes (A_2/M) are calculated at each temperature in accordance with Equation (1) by fitting the

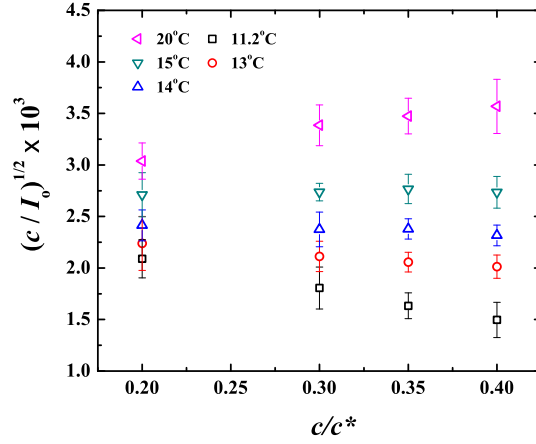


FIG. 4. Variation of reciprocal reduced intensity vs concentration . Slopes are calculated at each temperature by linear fitting of the data points.

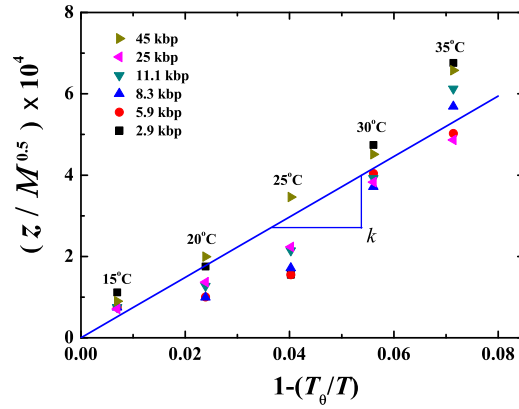


FIG. 5. Determination of the chemistry dependent constant k . The data points (except 114.8 and 289 kbp) are least square fitted with a straight line and the slope of this line gives k [Kumar and Prakash, 2003].

data points with straight lines and neglecting A_3 and the other higher order coefficients.

IX. DETERMINATION OF THE CHEMISTRY DEPENDENT CONSTANT k

The k value for the solvent has been determined by adopting a procedure elaborated in an earlier work [Kumar and Prakash, 2003], and briefly summarized in the main text (see Section III B).

Figure 5 displays plots of $f_g^{-1}(\alpha_g^{\text{expt}})/\sqrt{M}$ versus $\hat{\tau}$ for the solvent used in this study. Only the temperatures above the theta point are considered here. The data points were least square fitted with a straight line, and the slope k determined. θ -temperature value of 13°C has been used. The value of k found by this procedure is $7.4 \times 10^{-3} \pm 3.0 \times 10^{-4}$. However, while estimating the value of k , very high molecular weight linear DNA fragments (114.8 and 289 kbp) were not considered, since they deviated from the general behaviour. The reason for this could be that at high temperatures (30°C and 35°C), the high molecular weight linear DNA chains swell profusely and may start overlapping with each other (in a crossover region between dilute and semi-dilute solutions) resulting in solutions that may not be dilute in a physical sense.

REFERENCES

- Kumar, K. S. and J. R. Prakash, "Equilibrium swelling and universal ratios in dilute polymer solutions: Exact brownian dynamics simulations for a delta function excluded volume potential," *Macromolecules* **36**, 7842–7856 (2003).
- Laib, S., R. M. Robertson and D. E. Smith, "Preparation and characterization of a set of linear dna molecules for polymer physics and rheology studies," *Macromolecules* **39**, 4115–4119 (2006).
- Lewis, R. J., J. H. Huang and R. Pecora, "Rotational and translational motion of supercoiled plasmids in solution," *Macromolecules* **18**, 944–948 (1985).
- Orofino, T. A. and J. W. Mickey Jr., "Dilute solution properties of linear polystyrene in -solvent media," *J. Chem. Phys.* **38**, 2512–2520 (1963).
- Sambrook, J. and D. W. Russell, *Molecular Cloning: A Laboratory Manual (3rd edition)*, Cold Spring Harbor Laboratory Press, USA (2001).
- Selis, J. and R. Pecora, "Dynamics of a 2311 base pair superhelical dna in dilute and semidilute solutions," *Macromolecules* **28**, 661–673 (1995).
- Sorlie, S. S. and R. Pecora, "A dynamic light scattering study of four dna restriction fragments," *Macromolecules* **23**, 487–497 (1990).